OPTIMAL DESIGN OF A SINGLE PLATE CLUTCH FRICTION DISC USING ANSYS

By

Adarsh Venkiteswaran
Srinivasa V MuraliKrishna
Varun Subramoniam

MAE 598-2015-02
Final Report

ABSTRACT

The project presents a systematic approach to optimize the structural, thermal and vibrational characteristics of the clutch friction pad. A single plate clutch is modelled and analyzed using ANSYS. Thermal analysis considers the reduction of heat generated between the friction surfaces and reducing the temperature rise during the steady state period. Structural analysis is done to minimize the stresses developed as a result of the loading contact between friction surfaces. Also, modal analysis is done to optimize the natural frequency of the friction plate to avoid being in resonance with the engine frequency range. System Optimization is done using two methods to obtain a set of Pareto optimal points. Verifiable results are obtained through multi objective optimization namely MOGA and single objective optimization namely NLPQL.

Keywords: optimization, response surface optimization, Pareto optimal, multi-objective optimization.

Acknowledgement

We take immense pleasure in thanking Professor Dr. Max Yi Ren, Arizona State University, who had been a source of inspiration and providing his timely guidance and valuable inputs in the conduct of our Design Optimization project.

We also would like to thank staff of CAD/CAM Lab for providing us facilities to complete our project successfully.

To all our friends & family, we express our sincere gratitude for their moral support
Above all, we thank The Almighty, for giving us strength to finish the project.

Table of Contents

1 Design Problem Statement 9

2 General Nomenclature 10

3 Mathematical Calculations 10

4 Thermal Analysis 11

4.1 Nomenclature 11

4.2 Mathematical Calculations 12

5 Modal Analysis 12

5.1 Nomenclature 12

5.2 Mathematical Calculations 13

6 Model Analysis and Sub- System optimization Study 13

6.1 Design Variables 13

6.2 State Variables 13

6.3 Sub-system Optimization Process 14

6.3.1 Creation of Parametric model 15

6.4 Engineering Data 16

6.5 Geometry 16

6.6 FEM model 17

6.7 Objective functions 18

6.7.1 Modal Analysis 18

6.7.2 Structural Analysis 19

6.7.3 Thermal Analysis 21

6.8 Design of Experiments 23

6.9 Metamodeling 23

6.10 Response Surface Optimization 23

6.11 Parametric Study 24

6.11.1 Modal Analysis 24

6.11.2 Structural Analysis 26

6.11.3 Thermal Analysis 27

6.12 Discussion of Results 29

6.12.1 Modal Analysis (Vibrational Analysis) 29

6.12.2 Thermal Analysis 35

7 System Optimization 44

7.1 Multi-Objective Genetic Algorithm (MOGA) 45

7.1.1 Optimization Process 46

7.1.2 Results 46

7.2 Non-Linear Programming by Quadratic Lagrangian (NLPQL) 47

7.2.1 Optimization Process 47

7.2.2 Results 48

7.3 Conclusion 48

8 References 49

9 APPENDIX 50

Table of Figures

Figure 1: Clutch Assembly 9

Figure 2: Schematic Diagram of subsystem optimization in ANSYS 15.0 14

Figure 3: Subsystem Optimization Methodology 15

Figure 4: Parametric CAD model 17

Figure 5: ANSYS FEM model 17

Figure 6: Boundary conditions, fixed support 18

Figure 7: Rotational Velocity in Z direction 19

Figure 8: Clamping pressure load applied on the friction lining 20

Figure 9: Clutch lining constrained to rotate in Z direction only 20

Figure 10: Constraints applied on flywheel 21

Figure 11: Heat flux applied on the friction pads 22

Figure 12: Loads applied for heat dissipation 22

Figure 13: Frequency vs Lining Face Thickness 24

Figure 14: Frequency vs Lining Thickness 25

Figure 15: Frequency vs Lining Inner Diameter 25

Figure 16: Equivalent Stress vs lining face thickness 26

Figure 17: Equivalent Stress vs Lining Inner Diameter 26

Figure 18: Equivalent Stress vs Lining Thickness 27

Figure 19: Temperature vs Lining Inner Diameter 27

Figure 20: Temperature vs Lining Thickness 28

Figure 21: Temperature vs Lining Thickness 28

Figure 22: 668.67 Hz 30

Figure 23: 253.96 Hz 30

Figure 24: 167.44 Hz 30

Figure 25: 167.42 Hz 30

Figure 26: DOE samples 31

Figure 27: Optimized Design 32

Figure 28: Goodness of fit 33

Figure 29: Influence of parameters on output 33

Figure 30: Local Sensitivity Chart 34

Figure 31: Convergence Criteria 35

Figure 32: Temperature distribution at the end of slip time 35

Figure 33: DOE samples 36

Figure 34: Optimized Final Design 37

Figure 35: Optimized Input values 37

Figure 36: Goodness of fit 38

Figure 37: Influence of Parameter values 38

Figure 38: Sensitivity Chart 39

Figure 39: Covergence Criteria 39

Figure 40: Stress values at the end of slipping period 40

Figure 41: DOE Samples 41

Figure 42: Optimized Design 41

Figure 43: Goodness of Fit 42

Figure 44: Influence of Parameter values 43

Figure 45: Sensitivity Chart 43

Figure 46: Convergence Criteria 44

Figure 47: System Optimization schematic diagram 45

Figure 48: MOGA Pareto Surface 46

Figure 49: NLPQL Pareto Surface 48

1 Design Problem Statement

The primary aim of this work is to design a rigid drive clutch system that meets multiple objectives such as Vibrational rigidity, Structural and Thermal strength. Also, to demonstrate a systematic approach to solving multi-objective problems by Response Surface Optimization to obtain Pareto optimal solutions.

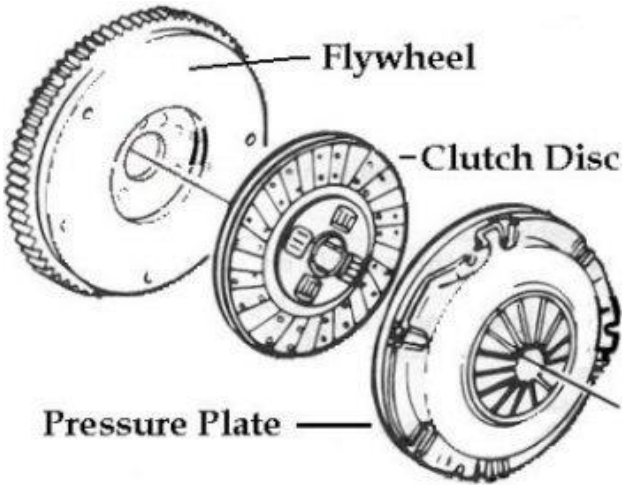

Figure 1: Clutch Assembly

Gradual engagement clutches like the friction clutches are widely used in automotive application for the transmission of torque from the flywheel to the transmission. The three major components of a clutch system are the clutch disc, the flywheel and the pressure plate. Flywheel is directly connected to the engine's crankshaft and hence rotates at the engine rpm. Bolted to the clutch flywheel is the second major component: the clutch pressure plate. The spring-loaded pressure plate has two jobs: to hold the clutch assembly together and to release tension that allows the assembly to rotate freely. Between the flywheel and the pressure plate is the clutch disc. The clutch disc has friction surfaces similar to a brake pad on both sides that make or break contact with the metal flywheel and pressure plate surfaces, allowing for smooth engagement and disengagement.

When the clutch begins to engage, the contact pressure between the contact surfaces will increase to a maximum value at the end of the slipping period and will continue to stay steady during the full engagement period. During the slipping period, large amount

of heat energy is generated at the contact surfaces, which gets converted to thermal energy by first law of thermodynamics. The heat generated is dissipated by conduction between the clutch components and convection to the environment. Another loading condition is the pressure contact between the contact surfaces that occurs due to the axial force applied the diaphragm spring. In addition to the above output responses, this work also considers the Vibrational characteristics of the clutch plate during the full engagement period. The engine and the transmission components experience dynamically varying loads during normal operation. This will cause vibrations and hence, one must design the clutch system so as to avoid resonance with the transmission and engine components.

2 General Nomenclature

P1 – Friction pad inner diameter

P2 – Friction pad thickness

P3 – Friction facing thickness

Ri – Inner radius of clutch disc in meters

Ro – Outer radius of the clutch disc in meters

N – Speed of engine in rpm = 3750 rpm

ω_r – angular velocity in rad/s

Pmax – clamping pressure in MPa

3 Mathematical Calculations

The material considered for the friction pad is Kevlar 49 Aramid. Uniform Wear Theory is considered for calculations, and accordingly, the intensity of the pressure is inversely proportional to the radius of friction plate.

$$R = \frac{Ri + Ro}{2} = 0.1m$$

In general, the frictional torque acting on the clutch plate is given by

$$T = N \times \mu \times W \times R$$

In general, the frictional torque acting on the clutch plate is given by W = 3000N

$$P \times r = C\ (constant)$$

Axial force on the clutch pad,

$$W = 2\pi \times C \times (Ro - Ri)$$

C = 0.0119Nm

The maximum pressure occurs at the inner radius and the minimum pressure at the outer radius.

In general, the frictional torque acting on the clutch plate is given by

$$Pmin = \frac{C}{Ro} = 0.0994\ Mpa$$

$$Pmax = \frac{C}{Ri} = 0.1492\ Mpa$$

Here, we consider the maximum pressure value obtained in the Finite Element Analysis of the clutch plate.

4 Thermal Analysis

4.1 Nomenclature

T – Temperature of the disc in Celsius

T_l – Limiting temperature of the material in Celsius = 150°C

μ - Coefficient of friction of the material = 0.4

k – Thermal conductivity of the material in Watts per meter Kelvin

h – Heat transfer coefficient of the material.in Watts per sq. meters per Kelvin.

q – Heat energy generated in watts

q_f – heat flux in W/m^2

t – Slip time in seconds = 0.5s

A – Area of a friction pad = $0.000931 m^2$

4.2 Mathematical Calculations

$$\omega_r = \frac{2 \times \pi \times N}{60} = 392.6\, rad/s$$

$$q = \mu \times Pmax \times \omega_r = 23.4375\, W$$

$$q_f = \frac{q}{A} = 25155\, W/m^2$$

5 Modal Analysis

5.1 Nomenclature

Fe – Engine frequency

n – Order of frequency (1st order & 2nd order)

Ne – Engine rpm range (1000 rpm-4750 rpm)

5.2 Mathematical Calculations

$$Fe = \frac{Ne}{60} \times n$$

6 Model Analysis and Sub- System optimization Study

6.1 Design Variables

Three design variables are chosen that will serve as constraints for all the three sub-systems. In a preliminary simulation study, it was observed that these parameters have a greater impact on the characteristics under study. Also, the rationale behind choosing wide range of values is to avoid excluding good designs.

$g1 : 140 \leq P1 \leq 160$

$g2 : \quad 2 \leq P2 \leq 10$

$g3 : \quad 0.5 \leq P3 \leq 3.5$

6.2 State Variables

The response quantities that are dependent on the above design variables are

1. Temperature
2. Vibration frequency
3. Equivalent Stress

6.3 Sub-system Optimization Process

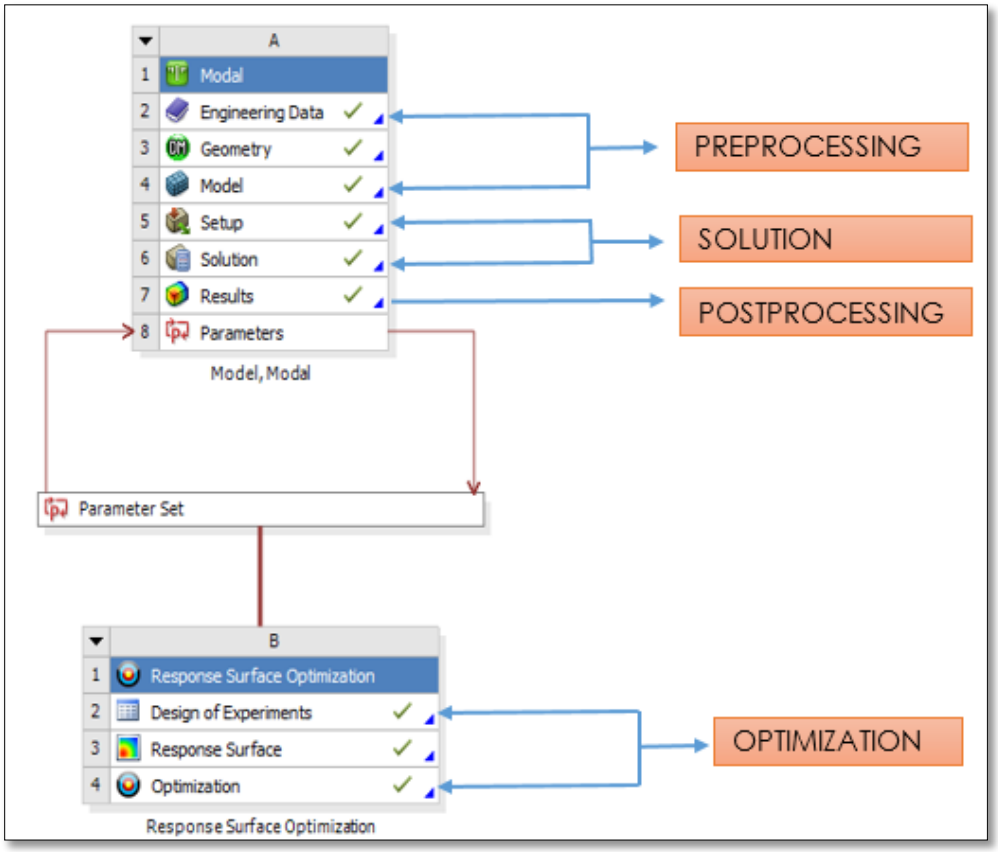

Figure 2: Schematic Diagram of subsystem optimization in ANSYS 15.0

The desired output response for each sub-system is obtained through Finite Element Analysis using ANSYS by selecting a parametric model with the design variables as input geometric parameters.

The following steps were sequentially carried out for each sub-system analysis and further for optimization.

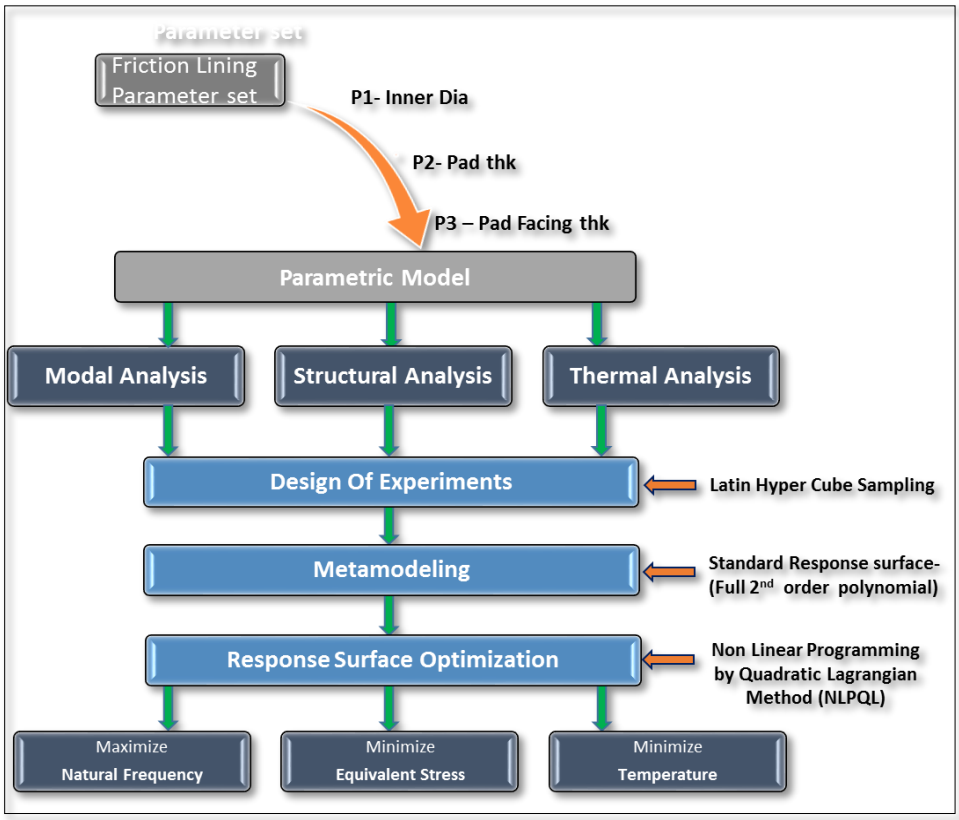

Figure 3: Subsystem Optimization Methodology

6.3.1 Creation of Parametric model

a. Create the CAD model for simulation using ANSYS Design Modeler.
b. Define the input parameters (Design Variables) to be investigated. The output parameters (State Variables) are chosen from the simulation results.
c. Define the design space by giving lower and upper bounds for the parameters and based on this the Design of Experiments (DOE) part will sample the design space.
d. Obtain an approximate response of the system by creating a Response Surface for each output parameter.
e. Repair errors to obtain an accurate response surface approximation.
f. Choose a suitable optimization technique after setting the constraints to finally identify suitable design candidates from the Response Surface.

6.4 Engineering Data

Engineering data involves defining clutch material and properties

Type	Clutch base plate	Clutch plate lining
Material	Structural Steel	Kevlar Aramide Fiber 49
Properties		
Density	7850	1440
Young's Modulus	2×10^{11} Pa	1.12×10^{11} Pa
Poisson's Ratio	0.3	0.36
Bulk Modulus	1.667×10^{11} Pa	1.333×10^{11} Pa
Shear Modulus	7.6923×10^{10} Pa	4.1176×10^{10} Pa
Specific heat Capacity	434 J kg^-1 C^-1	1420 J kg^-1 C^-1
Isotropic Thermal Conductivity	60.5 W m^-1 C^-1	0.04 W m^-1 C^-1

Table 1: Kevlar Aramid Fiber 49 properties

6.5 Geometry

The base dimensions for the model are

Parameter	Value
P1	160 mm
P2	2.7 mm
P3	0.8 mm

Table 2: Initial Input parameter values

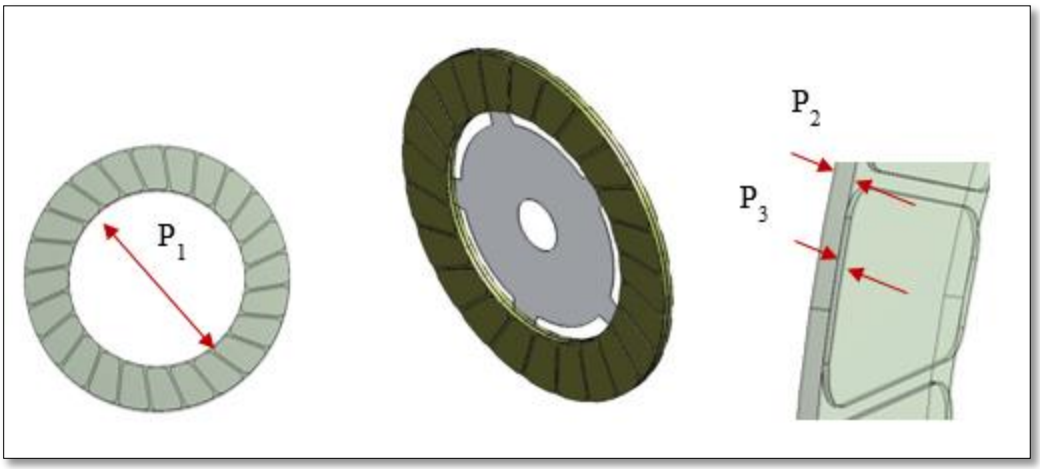

Figure 4: Parametric CAD model

6.6 FEM model

Meshing is an integral part of the FEA process. The mesh influences the accuracy, convergence and speed of the solution. A free mesh is applied with fine element size for the CAD model. A free mesh has no specific element shape or pattern associated with it.

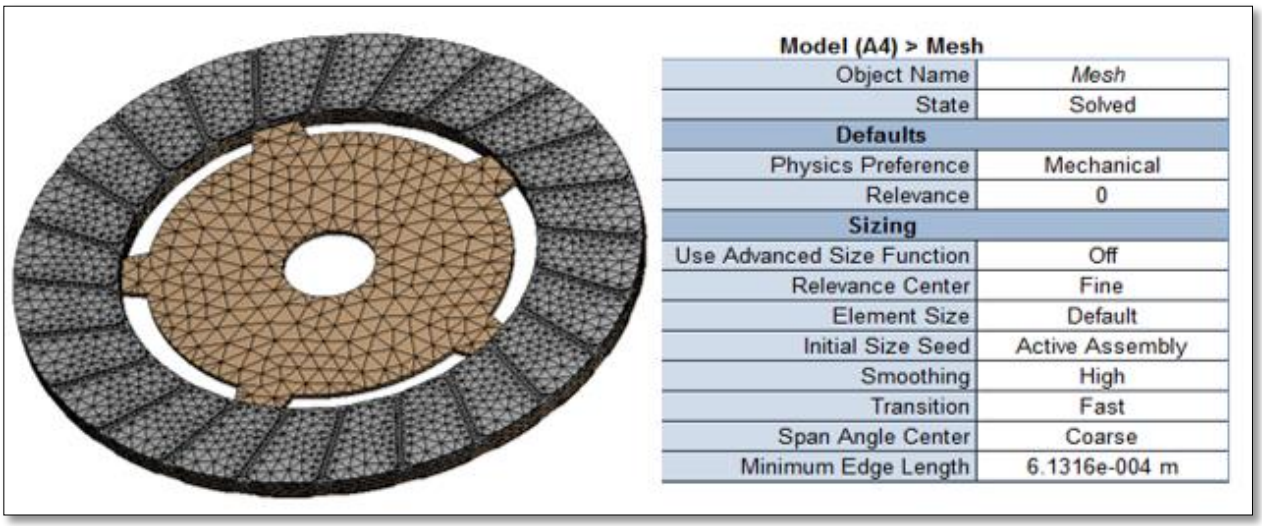

Model (A4) > Mesh

Object Name	*Mesh*
State	Solved
Defaults	
Physics Preference	Mechanical
Relevance	0
Sizing	
Use Advanced Size Function	Off
Relevance Center	Fine
Element Size	Default
Initial Size Seed	Active Assembly
Smoothing	High
Transition	Fast
Span Angle Center	Coarse
Minimum Edge Length	6.1316e-004 m

Figure 5: ANSYS FEM model

6.7 Objective functions

6.7.1 Modal Analysis

Maximize the 1st order frequency to avoid resonance with Engine and Transmission vibrations.

6.7.1.1 Boundary conditions & Loads

Since this is free vibration analysis, no external forces or loads were applied onto the FEM model. Practically, while measuring the clutch plate natural frequency, it is mounted on its base plate hole .In ANSYS simulation, the clutch plate given was fixed support constraint at its base plate hole diameter.

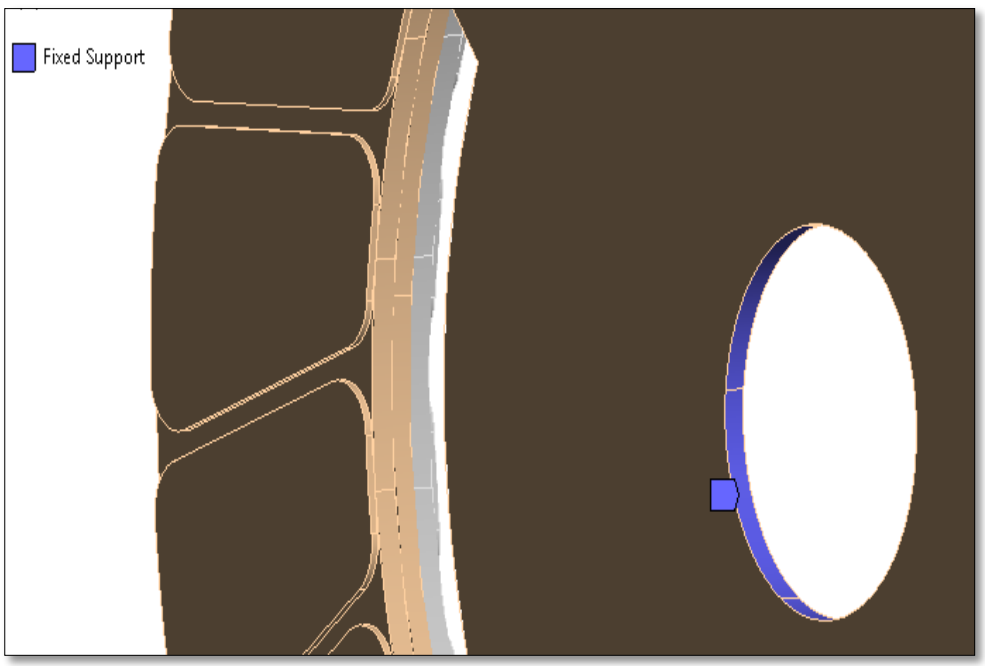

Figure 6: Boundary conditions, fixed support

6.7.2 Structural Analysis

Minimize the Max. Equivalent stress acting on the friction pad

6.7.2.1 Boundary conditions & loads

1) The relative rotational velocity between the clutch plate & flywheel for t = 0.5 s slip is applied on the clutch plate. Here the clutch plate is made to rotate with flywheel kept stationary.

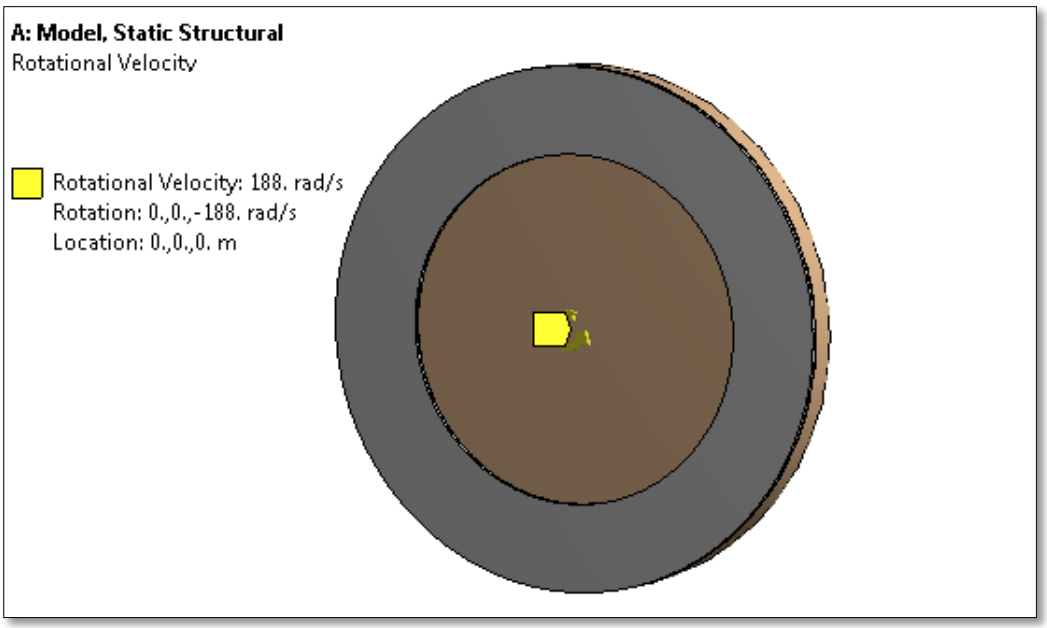

Figure 7: Rotational Velocity in Z direction

2) The contact pressure on clutch plate exerted by the pressure plate is applied on the clutch plate surface as per calculated value.

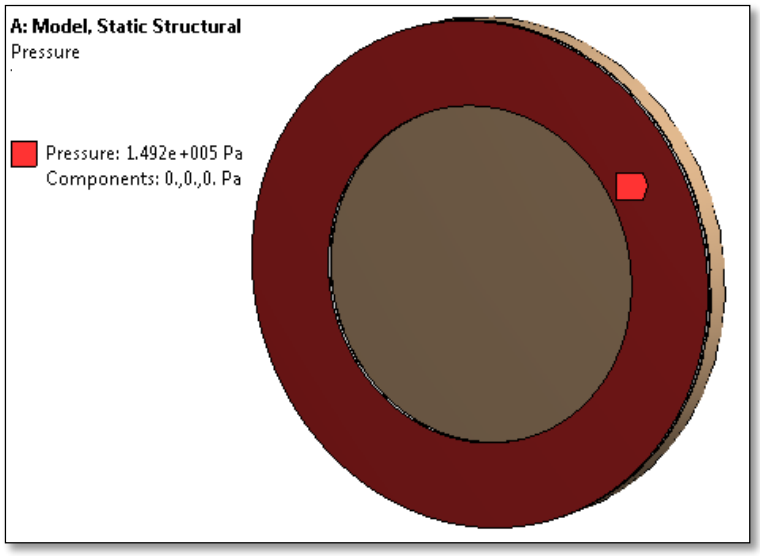

Figure 8: Clamping pressure load applied on the friction lining

3) The clutch plate is constrained to rotate only about Z direction.

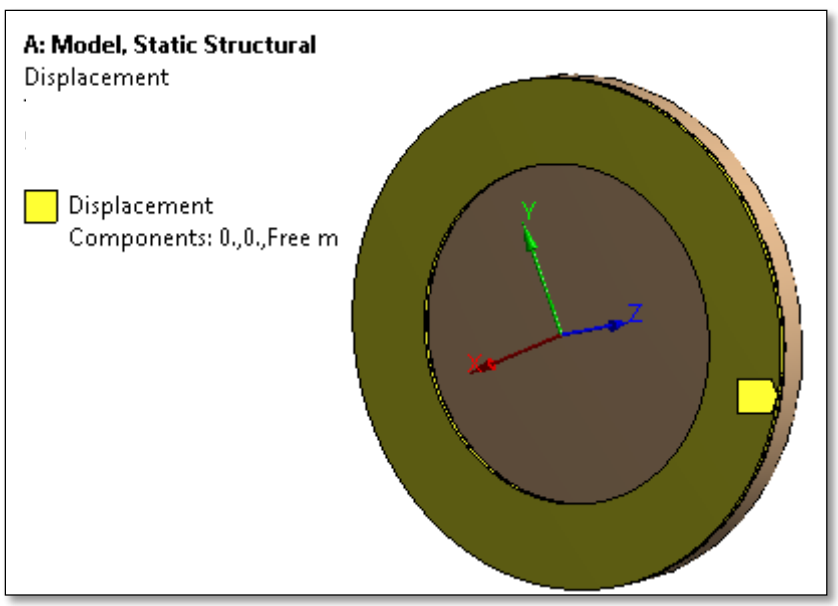

Figure 9: Clutch lining constrained to rotate in Z direction only

4) The flywheel is given fixed support constraint and is constrained for no rotation in all directions.

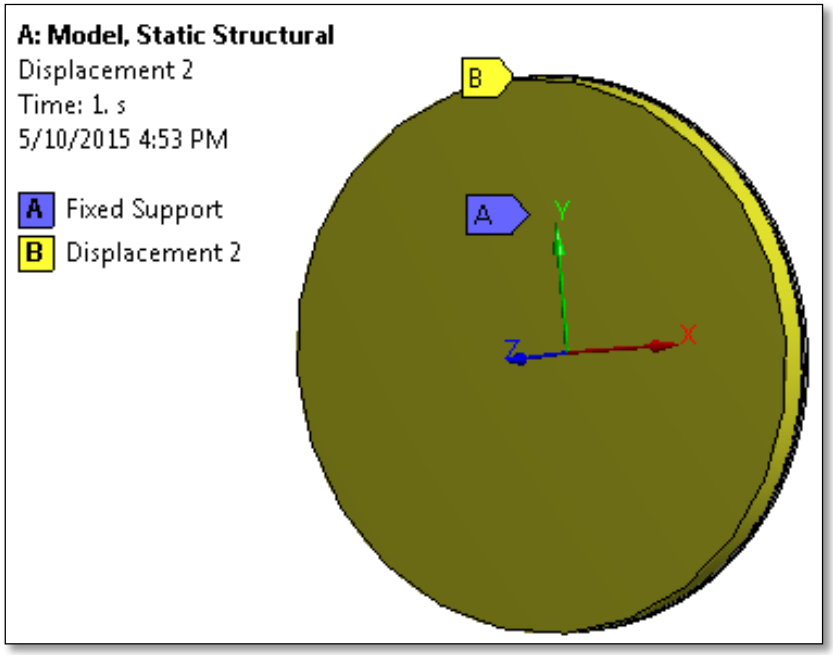

Figure 10: Constraints applied on flywheel

6.7.3 Thermal Analysis

Minimize the Max. Temperature due to the heat generated on friction pad

6.7.3.1 Boundary conditions & loads

1) During engagement of the clutches, the friction surface is in contact with the flywheel. The maximum heat flux of 25155 W/m^2 is applied onto the friction pads. The initial temperature for the analysis is set at ambient temperature (35 degree Celsius).

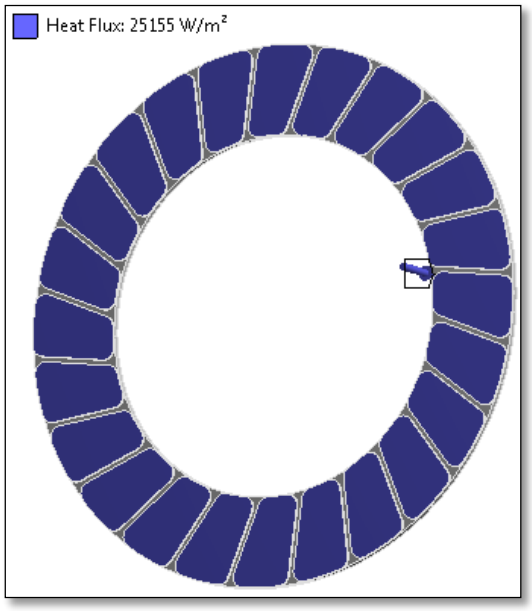

Figure 11: Heat flux applied on the friction pads

2) The heat generated by the clutch engagement is dissipated through convection and radiation. A convective heat transfer coefficient of 40 W/m^2 (of free air) is applied. For radiation 35 degree Celsius was applied

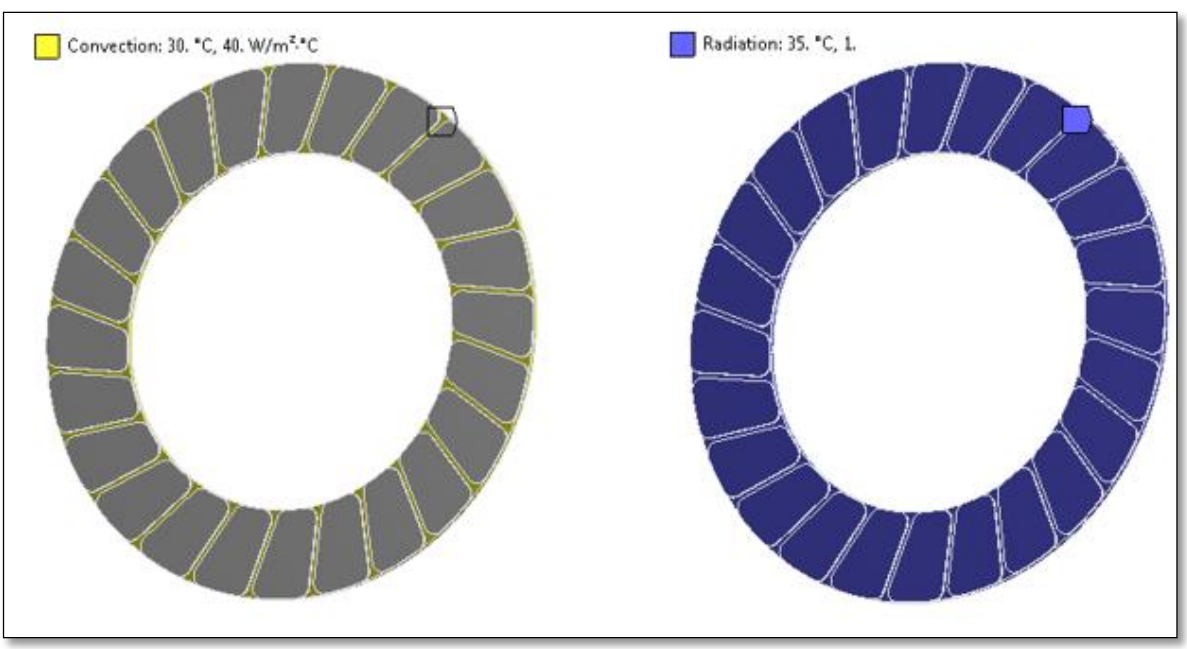

Figure 12: Loads applied for heat dissipation

6.8 Design of Experiments

The next step is to establish a relationship between the design variables and the output response. Since all the design variables are continuous within their bounds, one needs to sample the design space to determine how many and which parameters should be chosen for creating a response surface. Here, the widely used stochastic sampling technique, Latin Hypercube Sampling (LHS) is adopted. A set of *l* samples are randomly generated regardless of the number of design variables. The advantage of LHS is that the samples do not share the same values on any variable and hence offers a good distribution in the design space. Also, unlike other deterministic methods like Central Composite Design (CCD) and Full factorial methods, the number of simulations required for LHS remain constant (after converging to a maximum) even with an increasing number of parameters. At the end of this stage, output parameters corresponding to the design points as defined by the DOE is obtained.

6.9 Metamodeling

Further, using metamodeling (regression analysis) techniques, a response surface that provides a functional relationship between the output response and the input parameters is generated. A full second order polynomial is the preferred model and uses the method of least squares to determine the value of the unknown coefficients A, B and C in the second order polynomial, $Ax^2 + Bx + C$. The advantage of nonlinear least squares regression like the second order polynomial over many other techniques is the broad range of functions that can be fit.

6.10 Response Surface Optimization

Now that the meta-model of the problem has been developed, gradient-based methods can be applied to search for the optimal point in the response surface. When the design variables are continuous and the optimization is single objective, NLPQL (Non-Linear Programming with Quadratic Lagrangian) is a very efficient algorithm. NLPQL uses quasi-Newton methods to converge to the solution. It generates a sequence of QP sub-

problems which is obtained by quadratic approximation of the Lagrangian function and linearization of constraints. And finally, to stabilize and ensure global convergence, an Armijo line-search is performed.

Once the response surface optimization is completed, a manual refinement of the response surface is done by inputting the optimal point as a design point and re-solving the optimization problem until a good approximation of the actual response is obtained.

6.11 Parametric Study

The effect of input parameters on output parameter is studied from design sample space and the variation of output parameter against each input parameter is plotted

6.11.1 Modal Analysis

Below graphs show the response in frequency with the change in input parameters.

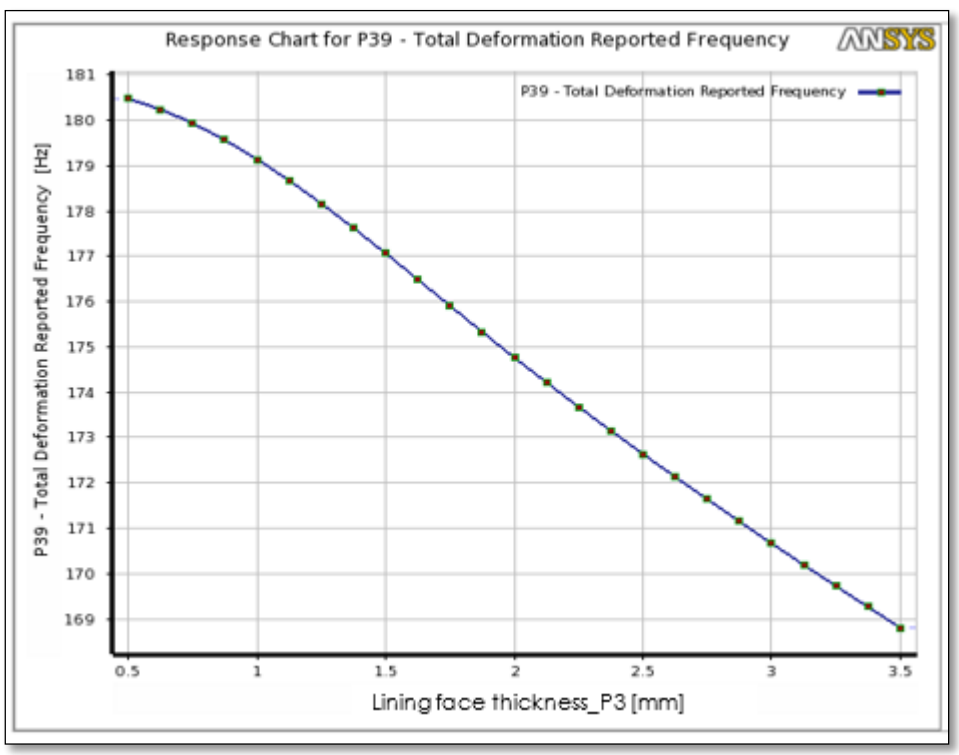

Figure 13: Frequency vs Lining Face Thickness

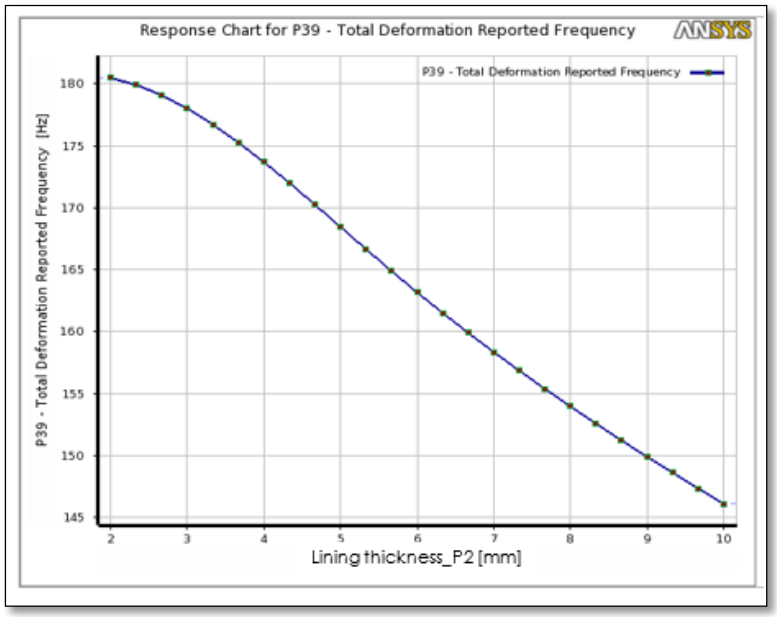

Figure 14: Frequency vs Lining Thickness

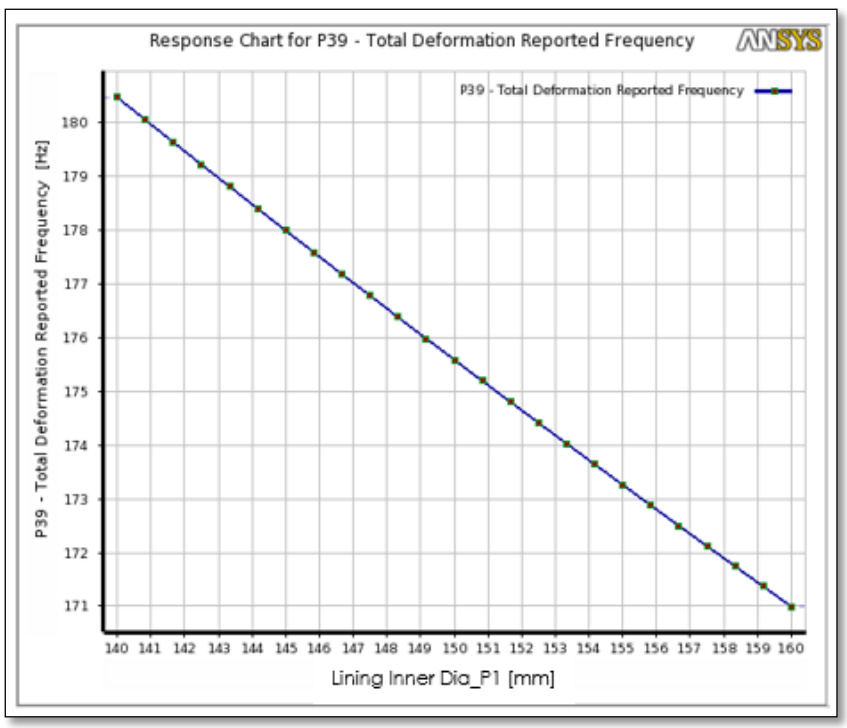

Figure 15: Frequency vs Lining Inner Diameter

6.11.2 Structural Analysis

Below graphs show the response in equivalent stress with the change in input parameters.

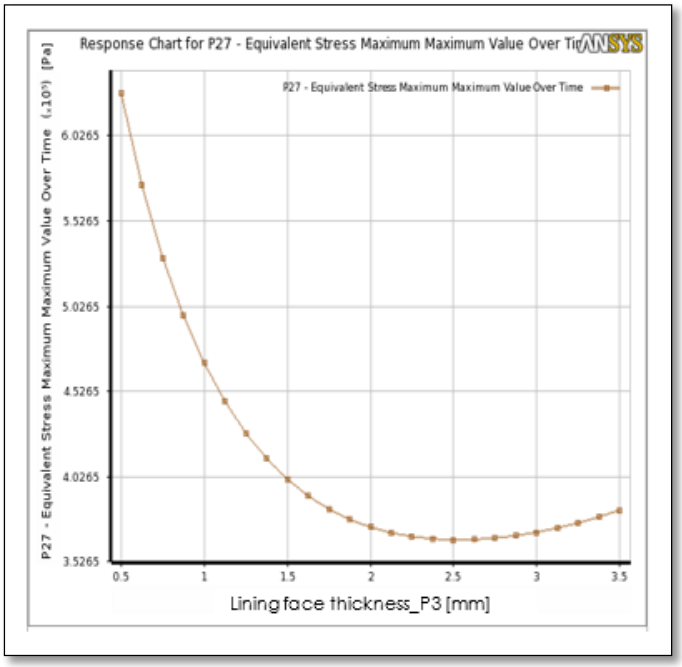

Figure 16: Equivalent Stress vs lining face thickness

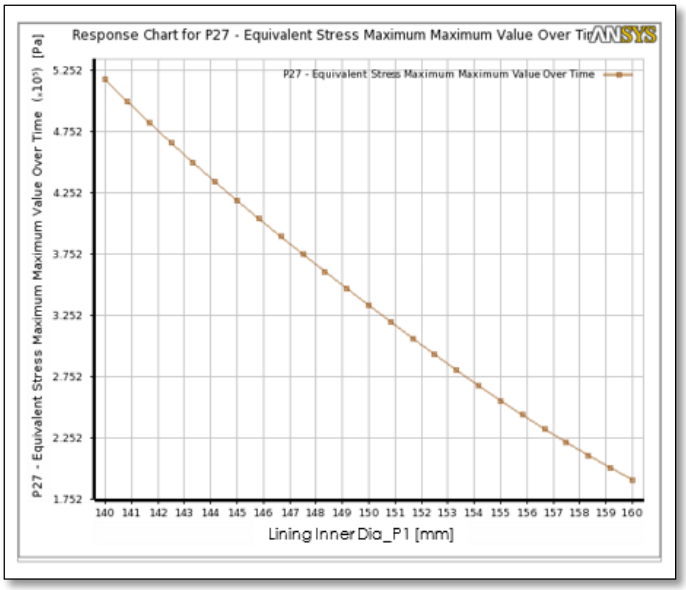

Figure 17: Equivalent Stress vs Lining Inner Diameter

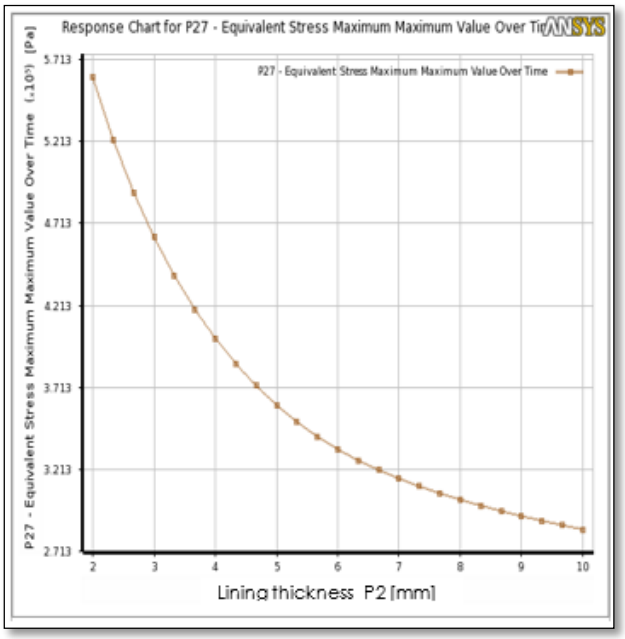

Figure 18: Equivalent Stress vs Lining Thickness

6.11.3 Thermal Analysis

Below graphs show the response in maximum temperature with the change in input parameters.

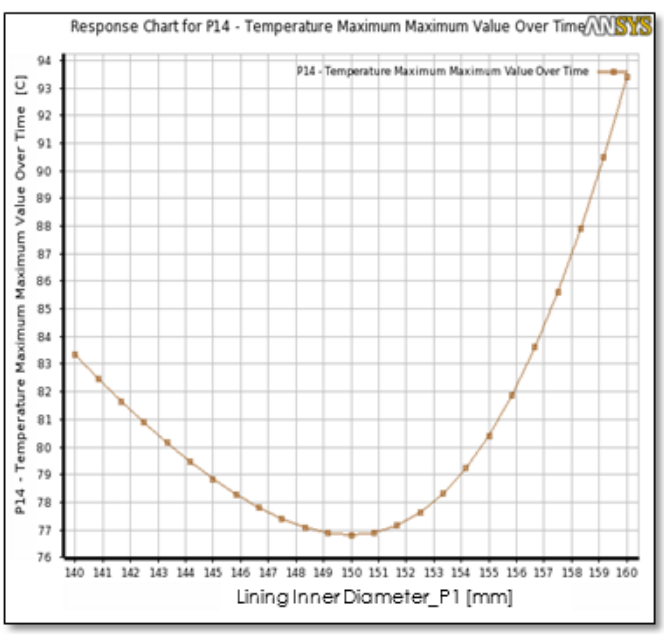

Figure 19: Temperature vs Lining Inner Diameter

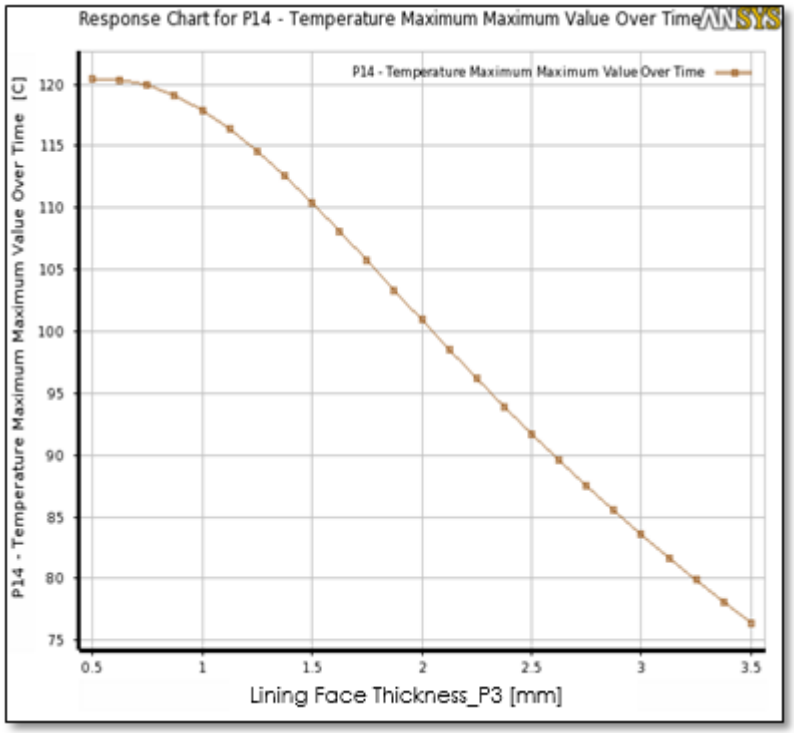

Figure 20: Temperature vs Lining Thickness

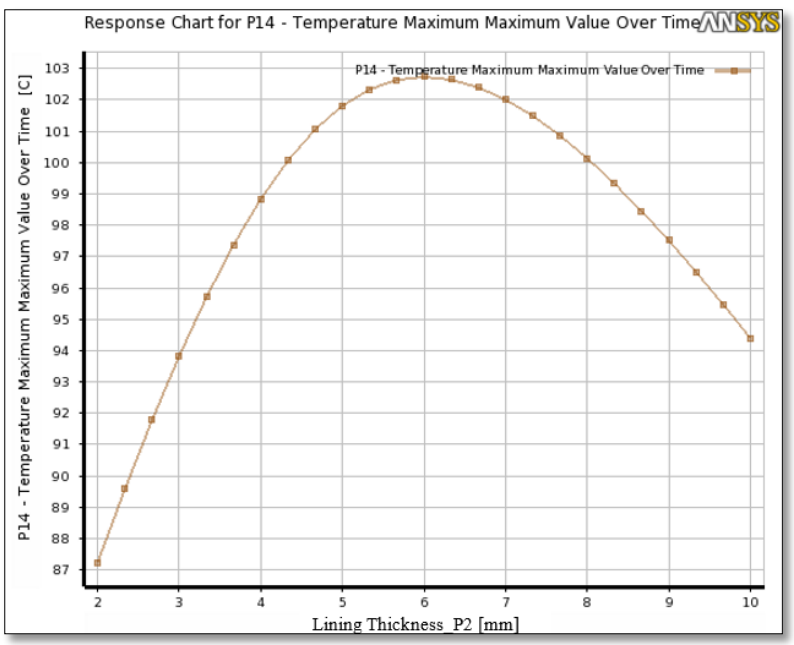

Figure 21: Temperature vs Lining Thickness

6.12 Discussion of Results

6.12.1 Modal Analysis (Vibrational Analysis)

The basic equation solved in a typical undamped modal analysis is the classical Eigen value problem

$$[\boldsymbol{K}]\{\emptyset_{\boldsymbol{I}}\} = \boldsymbol{\omega_i}^2[\boldsymbol{M}]\{\emptyset_{\boldsymbol{I}}\}$$

Where

$[\boldsymbol{K}]$ = Stiffness matrix

$\{\emptyset_{\boldsymbol{I}}\}$= Mode shape vector (Eigen vector) of mode

$\boldsymbol{\omega_i}$ = Eigen value

Ω =Natural circular frequency

By default, ANSYS Mechanical APDL uses Block Lanczos Mode Extraction Method to extract modes

Following natural frequencies are reported after simulation

Mode	Frequency[Hz]
1	167.42
2	167.44
3	253.96
4	668.67

Table 3: Frequency response

The mode shapes are

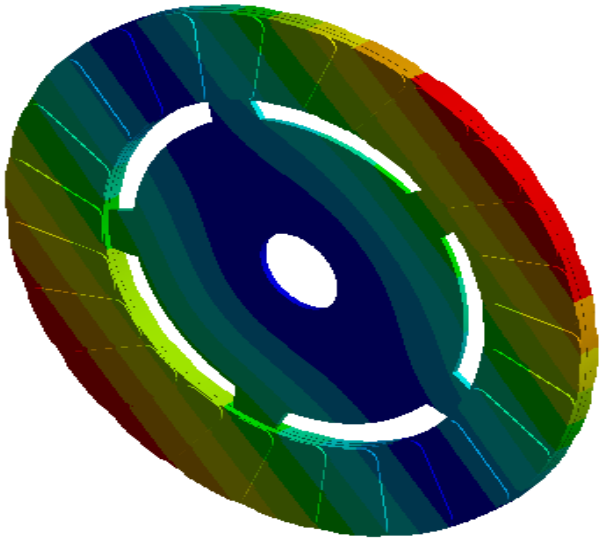

Figure 24: 167.44 Hz

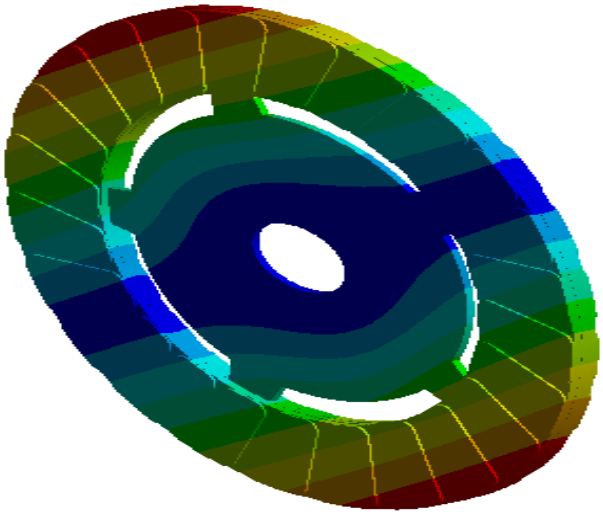

Figure 25: 167.42 Hz

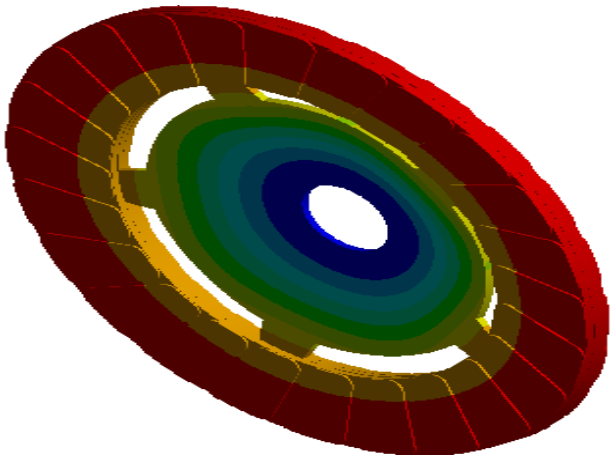

Figure 23: 253.96 Hz

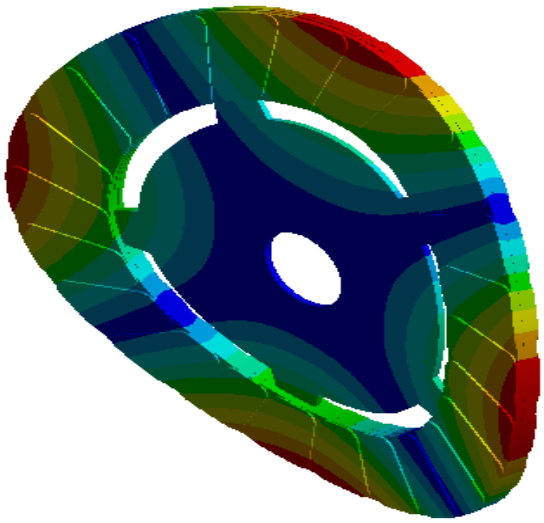

Figure 22: 668.67 Hz

The engine rpm range is from 1000 rpm (idling speed) to 4750 rpm (engine fly-up rpm).Taking into standard operating tolerance of 10% on the frequency range, the corresponding 1st order frequency range is **18.326 Hz- 87.076 Hz** and 2nd order frequency ranges **36.663 Hz -174.163 Hz**. These are the frequency bands with which clutch plate frequency should be decoupled.

Here, the first mode frequency is considered as the output parameter for optimization as it is the fundamental natural frequency. The 1st natural frequency (167.42 Hz) needs to be optimized so that it doesn't fall into the engine frequency band thereby avoid resonance.

6.12.1.1 Optimization Results

The NLPQL optimization is based on the response surface generated by regression analysis of design sample space as defined by below design points

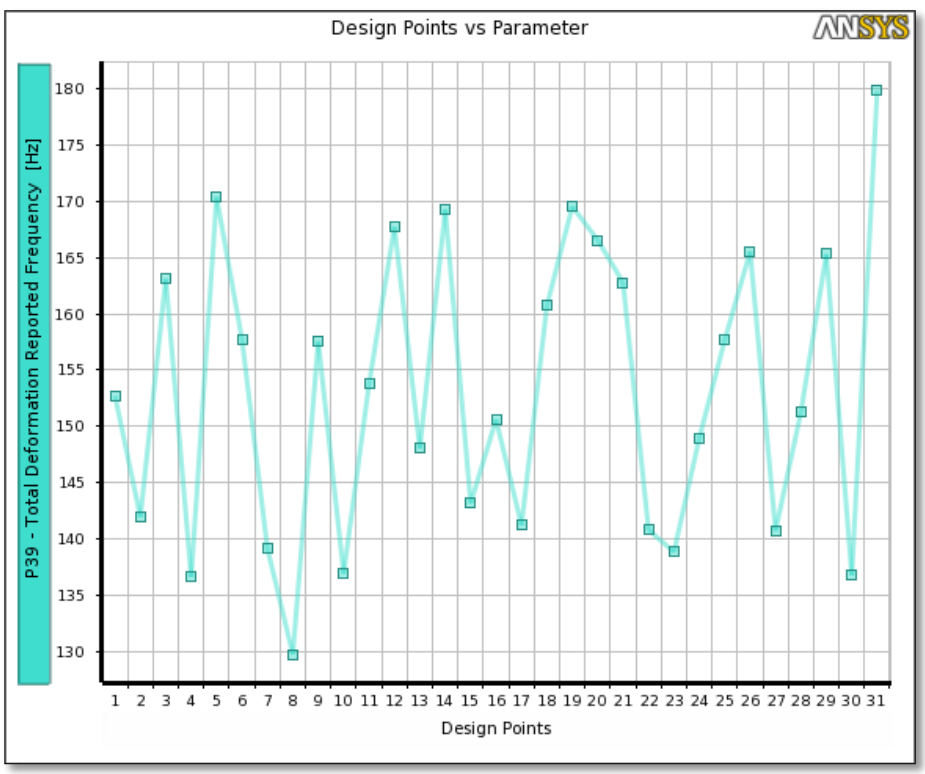

Figure 26: DOE samples

With optimization, there is 7.42 % improvement in the output frequency which doesn't fall in engine frequency band.

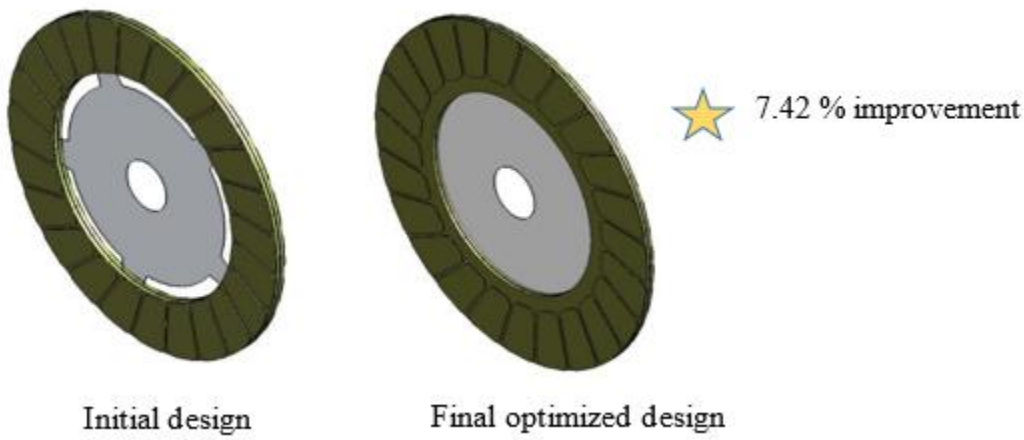

Figure 27: Optimized Design

Parameter	Starting Point	Final Design	
P1 (mm)	160	140 **(active)**	
P2 (mm)	2.7	2 (**active)**	
P3 (mm)	0.8	0.5 **(active)**	
Output	Initial Value	Optimized Value	Simulated Value
Frequency (Hz)	167.42	180.47	179.85

Table 4: Optimized Input Parameter Values

The above table shows the predicted value from NLPQL and observed value from ANSYS Simulation are very close enough.

6.12.1.1.1 Robustness of Solution (Goodness of Fit)

Goodness of Fit shows that the output parameter has been very well approximated by the response surface. The coefficient of determination is 0.99876.

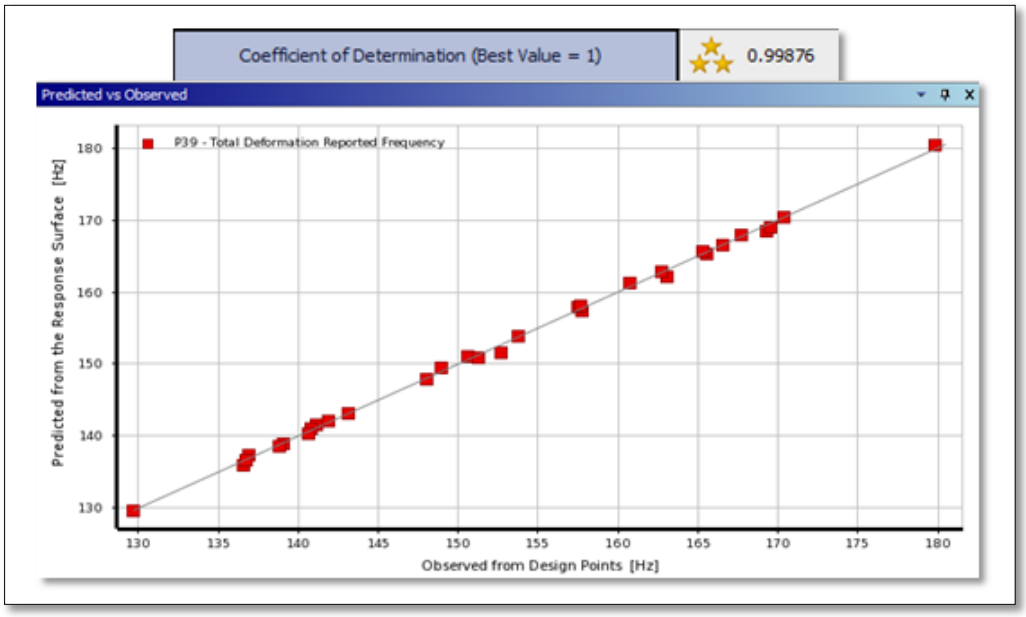

Figure 28: Goodness of fit

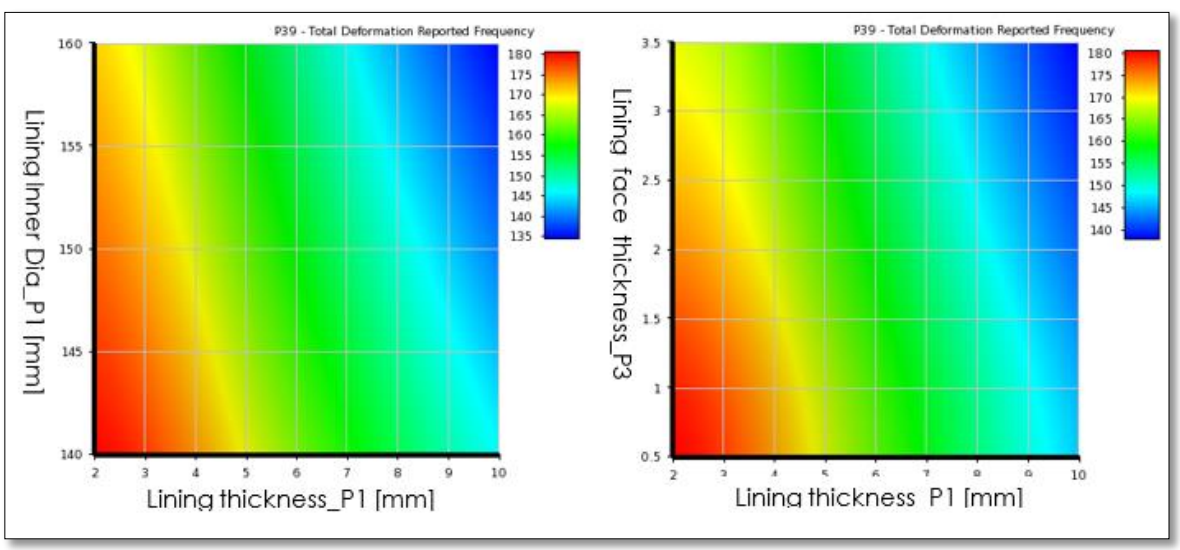

Figure 29: Influence of parameters on output

From the above contour plots for output frequency vs Input Parameters, it can be seen that the at the lower bound of all the constraints g1,g2 &g3,the function is monotonically increasing and the constraints are active.

The output frequency can be maximized further if the lower bound of constraints are relaxed.

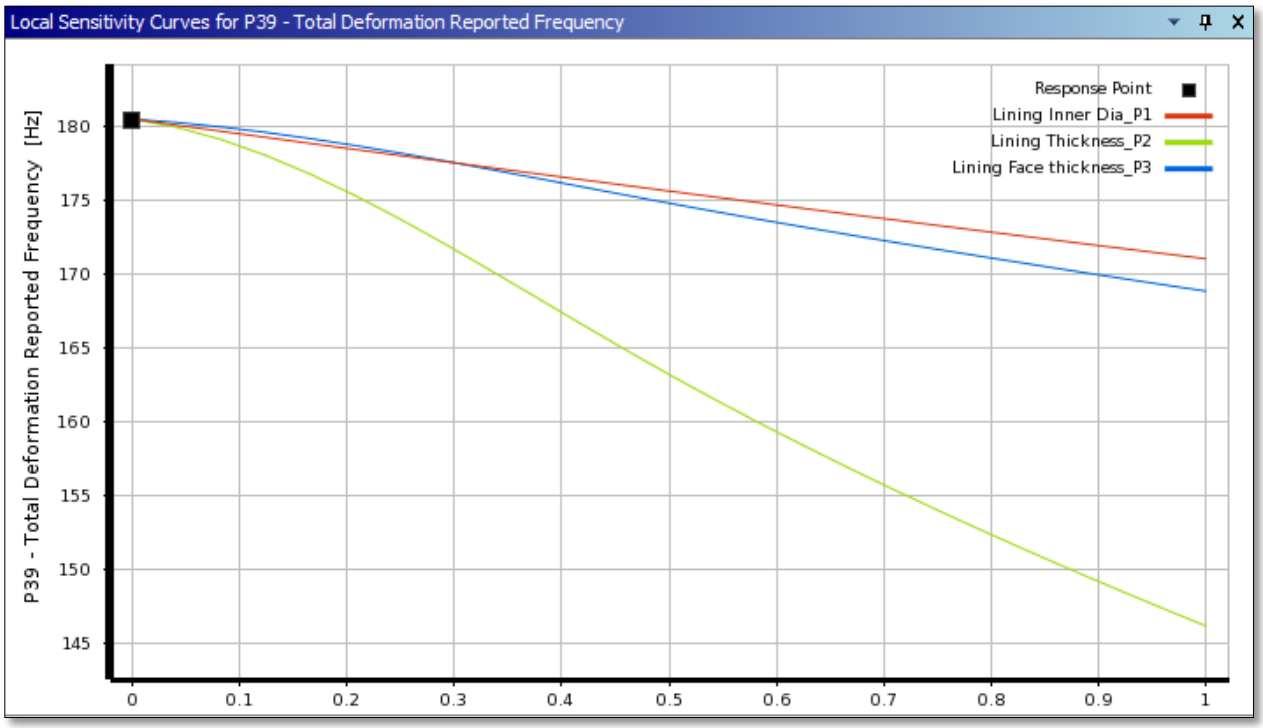

Figure 30: Local Sensitivity Chart

Local Sensitivity Curve shows the impact of each input parameter on output.

Convergence Criteria shows the no. of Iterations required to achieve optimal solution

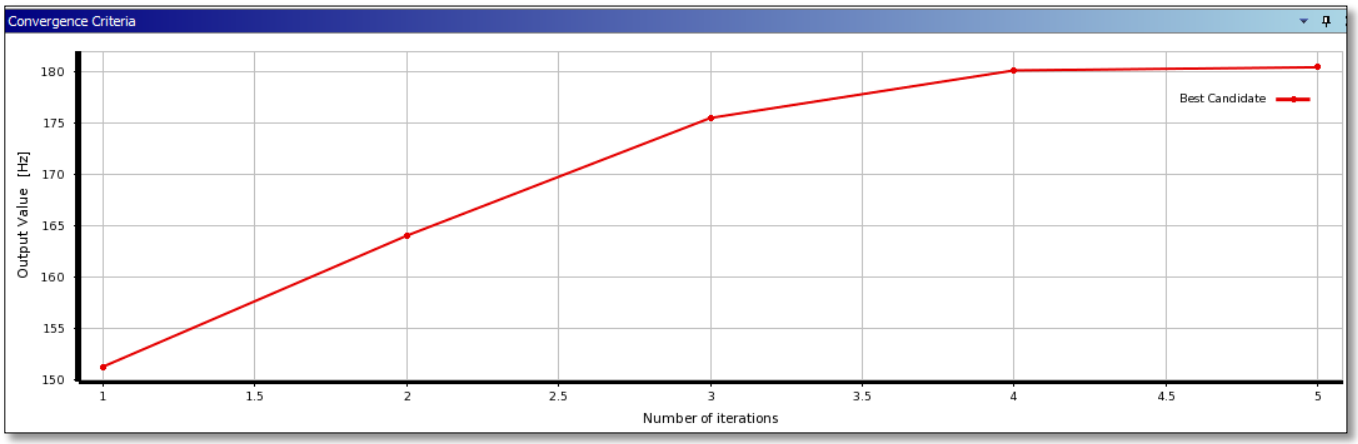

Figure 31: Convergence Criteria

6.12.2 Thermal Analysis

The change in maximum temperature with respect to time on application of the heat flux and other loads is as shown below. The maximum temperature reached with the initial design at the end of 0.5 seconds, the slip time, is 109.9 degree Celsius

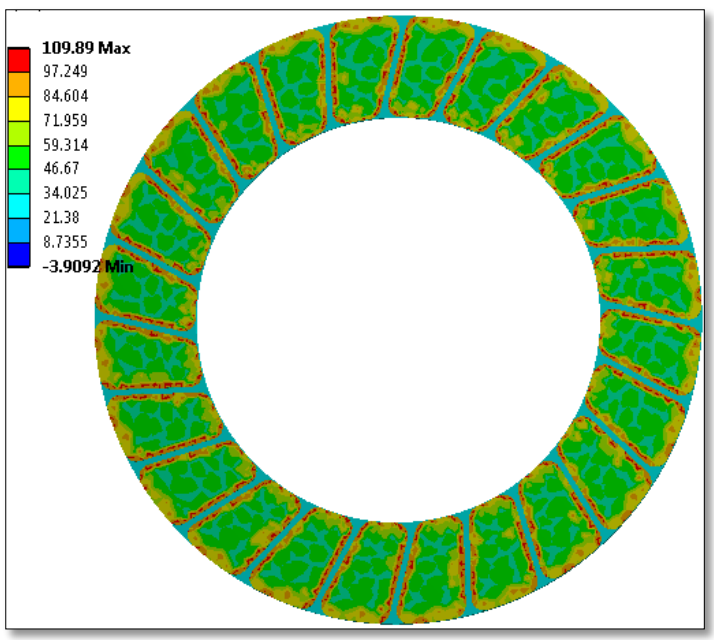

Figure 32: Temperature distribution at the end of slip time

This output maximum temperature has to be minimized so as to avoid the failure of friction pad material due to repeated clutch engagements lowering its cooling period

6.12.2.1.1 Optimization Results

The NLPQL optimization is based on the response surface generated by regression analysis of design sample space as defined by below design points.

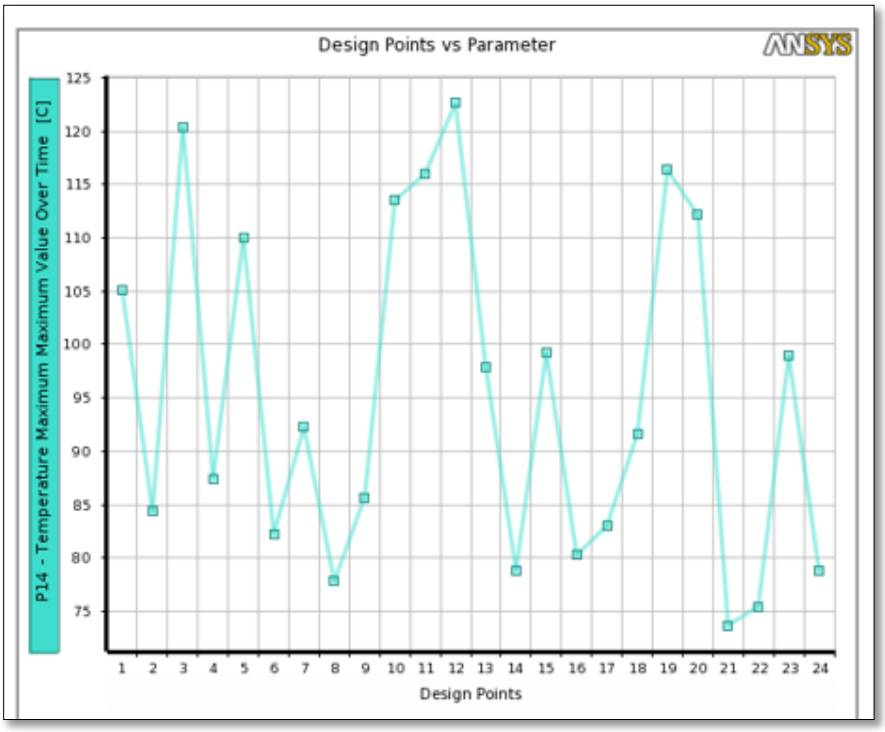

Figure 33: DOE samples

With optimization, there is 31.3 % improvement in the output frequency which doesn't fall in engine frequency band.

Figure 34: Optimized Final Design

Parameter	Starting Point	Final Design	
P1 (mm)	160	150	
P2 (mm)	2.7	6	
P3 (mm)	0.8	3.5 **(active)**	
Output	Initial Value	Optimized Value	Simulated Value
Temperature(°C)	109.9	76.79	75.46

Figure 35: Optimized Input values

Robustness of Solution (Goodness of Fit)

Goodness of Fit shows that the output parameter has been very well approximated by the response surface .The coefficient of Determination is 0.92091

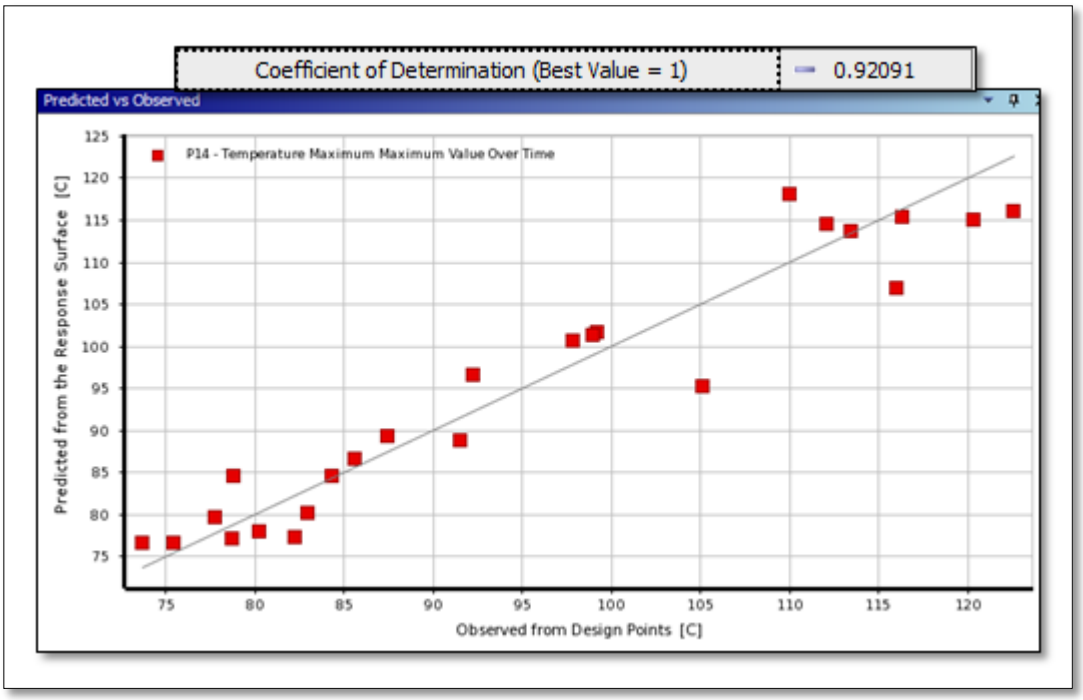

Figure 36: Goodness of fit

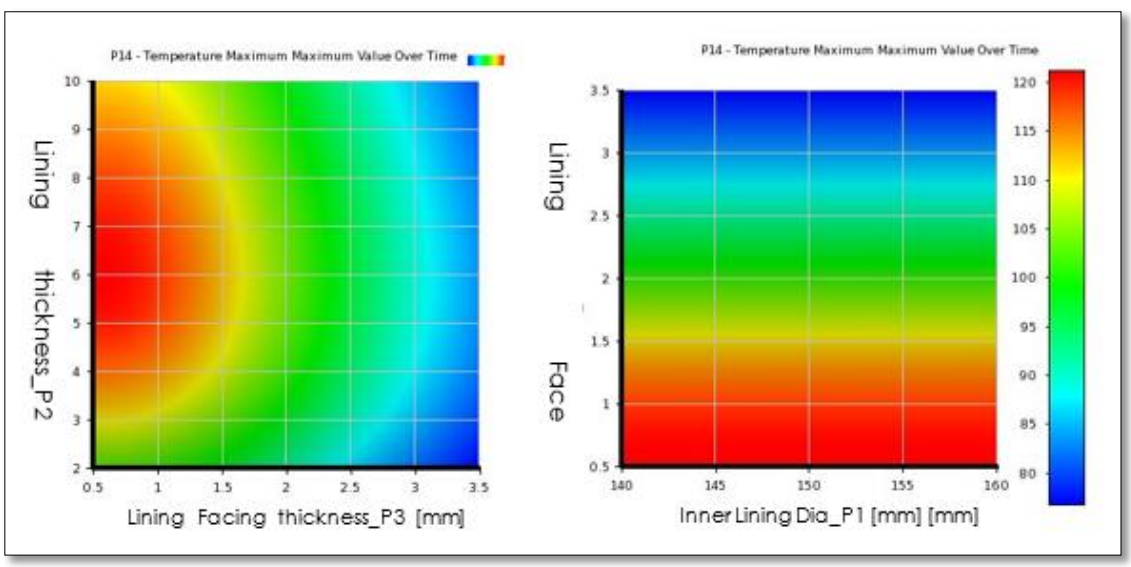

Figure 37: Influence of Parameter values

From the above contour plots for Maximum temperature vs Input Parameters, it can be seen that at the upper bound of the constraints g3, the function is monotonically decreasing and the constraints is active from upper bound.

Local Sensitivity Curve shows the impact of each input parameter on output.

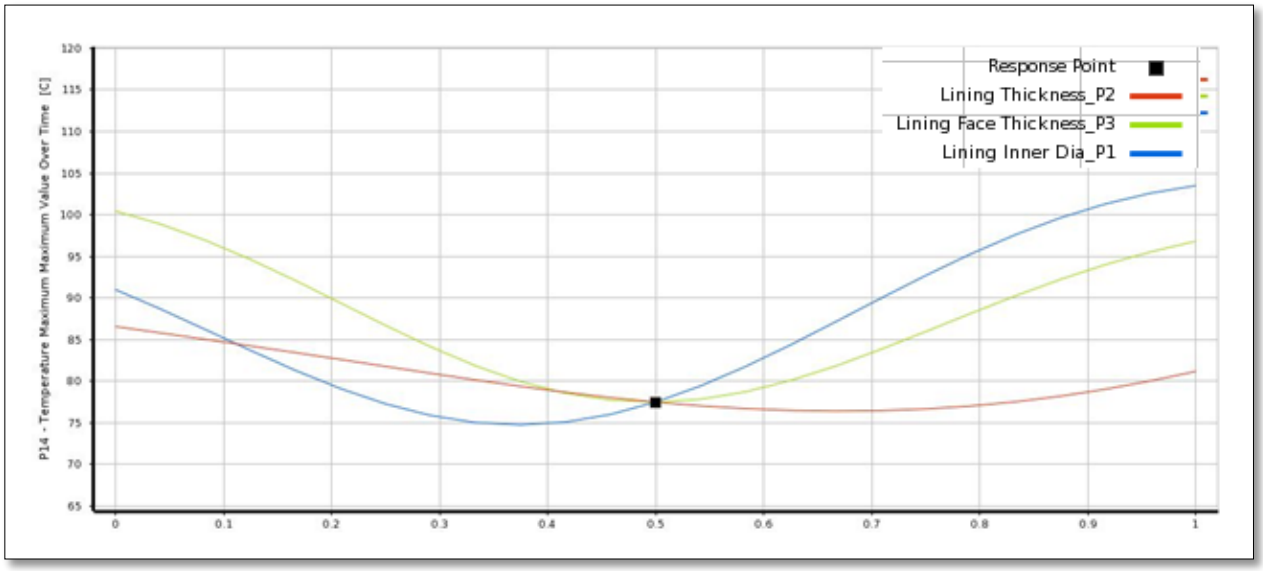

Figure 38: Sensitivity Chart

Convergence Criteria shows that two Iterations are required to achieve optimal temperature.

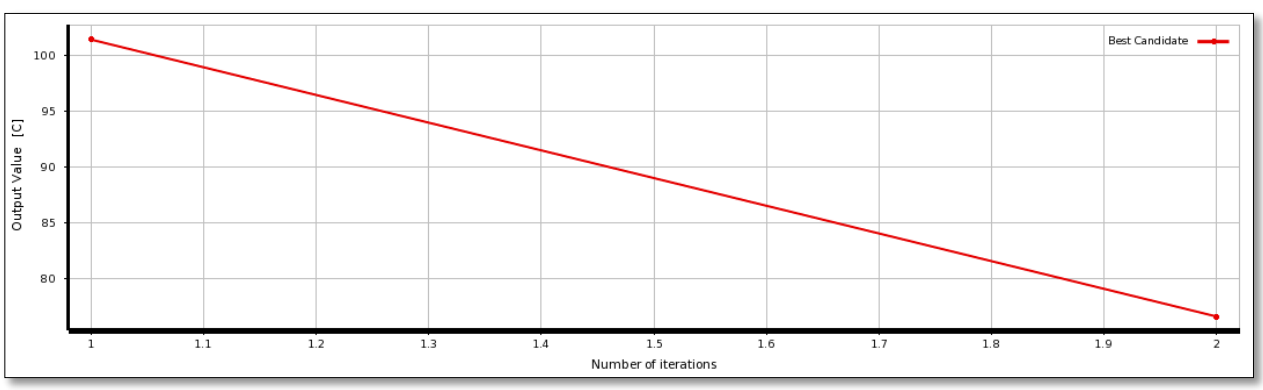

Figure 39: Covergence Criteria

Structural Analysis

The Equivalent Stress reached with the initial design at the end of 0.5 seconds, the slip time, is 2.5452e5 Pa.

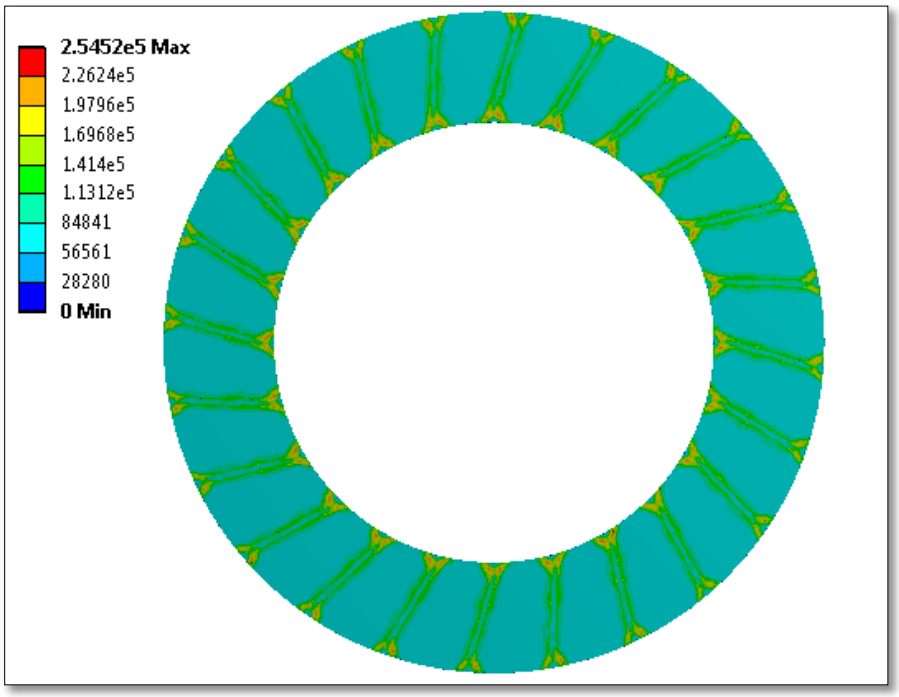

Figure 40: Stress values at the end of slipping period

This equivalent stress has to be minimized so as to avoid clutch plate failure

Optimization Results

The NLPQL optimization is based on the response surface generated by regression analysis of design sample space as defined by below 30 design points

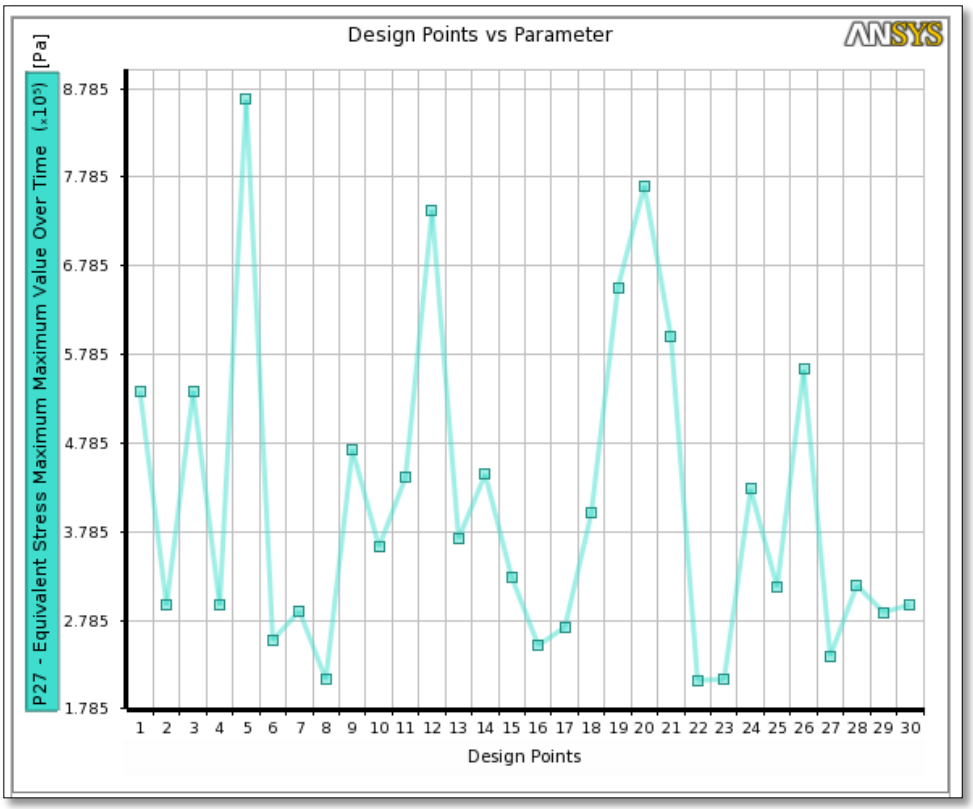

Figure 41: DOE Samples

With optimization, there is 27.61 % improvement in the output frequency which doesn't fall in engine frequency band.

Figure 42: Optimized Design

Parameter	Starting Point	Final Design	
P1 (mm)	160	160**(active)**	
P2 (mm)	2.7	10**(active)**	
P3 (mm)	0.8	2.52	
Output	**Initial Value**	**Optimized Value**	**Simulated Value**
Stress(MPa)	0.254	0.18	0.185

Table 5: Optimized Input parameter values

The above table shows the predicted value from NLPQL and observed value from ANSYS simulation are very close enough.

Robustness of Solution (Goodness of Fit)

Goodness of Fit shows that the output parameter has been very well approximated by the response surface .The coefficient of Determination is 0.98149

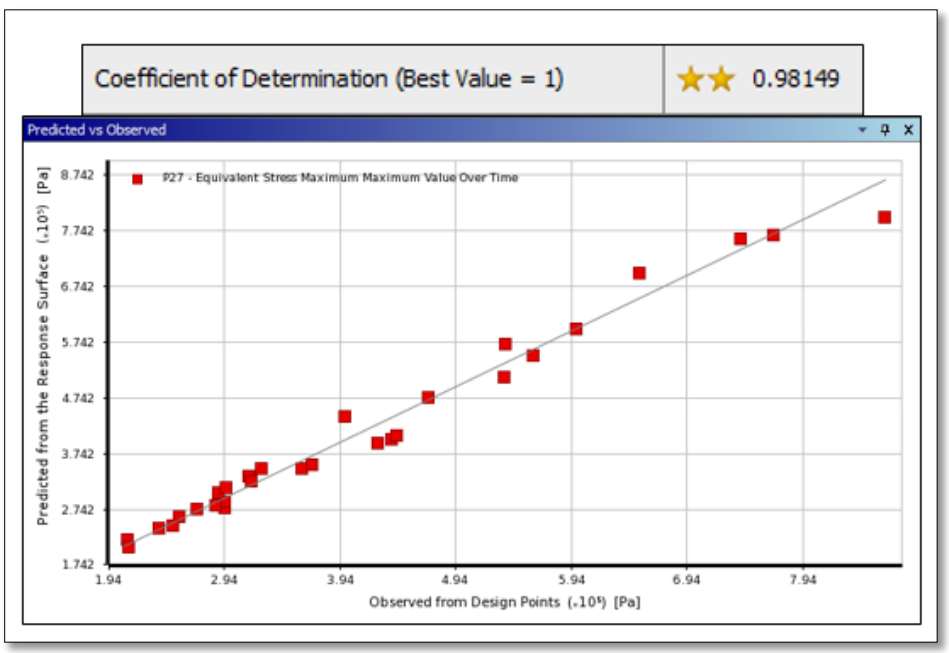

Figure 43: Goodness of Fit

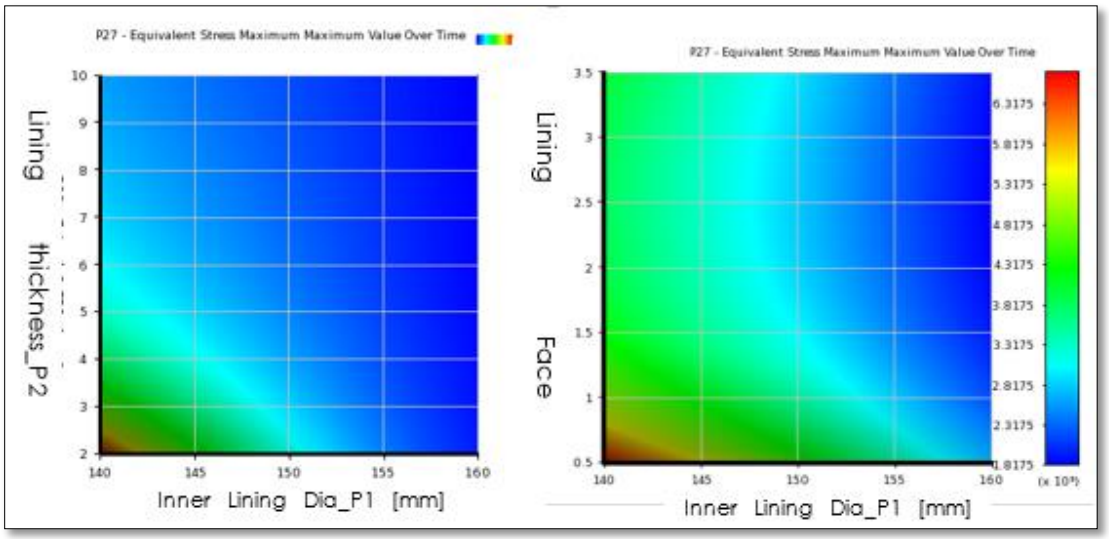

Figure 44: Influence of Parameter values

From the above contour plots for Equivalent Stress vs Input Parameters, it can be seen that at the upper bound of the constraints g1 & g2, the function is monotonically decreasing and the constraints are active from upper bound.

Local Sensitivity Curve shows the impact of each input parameter on output

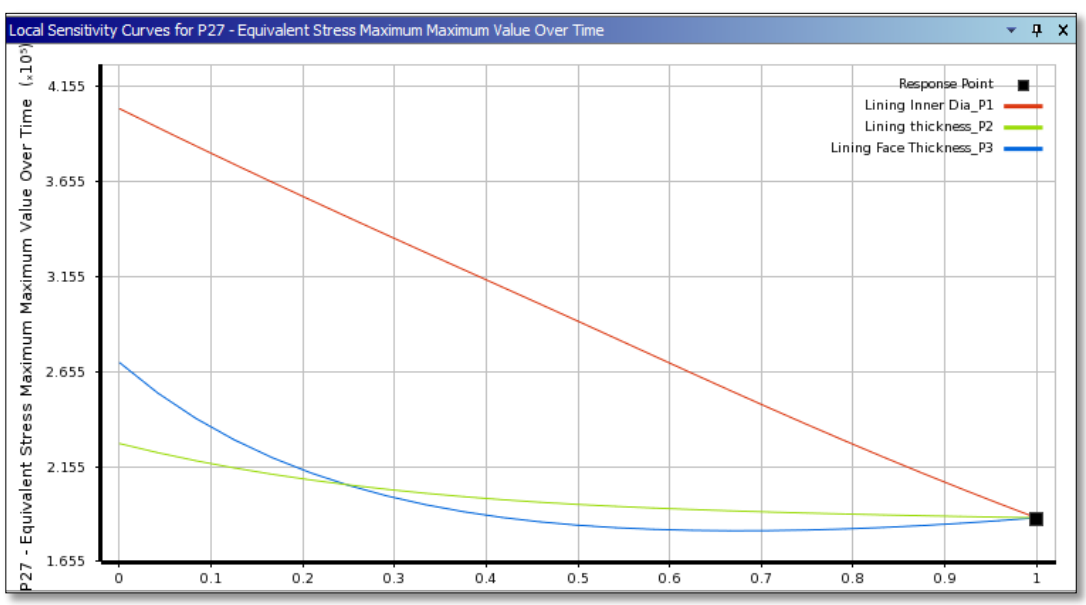

Figure 45: Sensitivity Chart

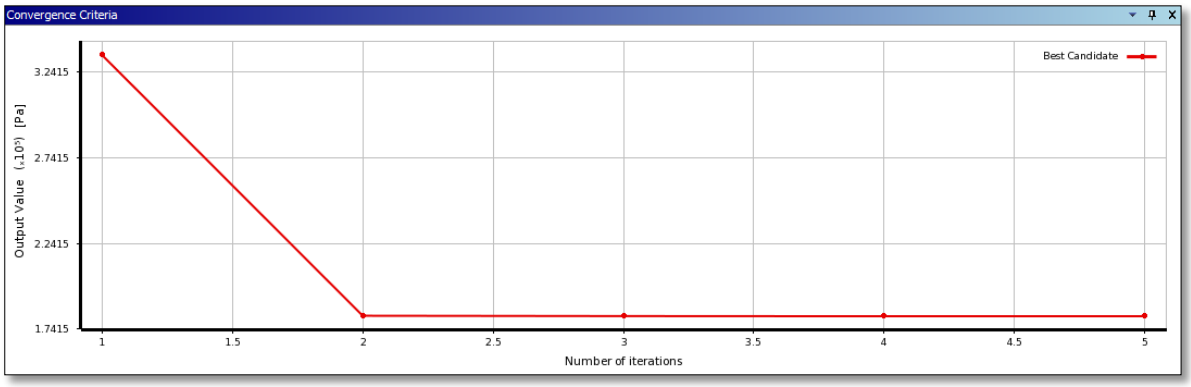

Figure 46: Convergence Criteria

Convergence Criteria shows that five Iterations are required to achieve optimal temperature.

7 System Optimization

System optimization is basically the process of enhancing the capabilities of a system by integrating the subsystems of which the former is made to the extent that all of them operate above the user expectations. In the project of optimizing the clutch design, the optimized subsystems viz. Modal Analysis, Structural Analysis and Thermal Analysis are integrated to create an optimal Pareto surface. A Pareto surface is the surface containing optimal points corresponding to the optimal solution of a particular trade-off among the conflicting objectives of the subsystem. In other words, selecting one point from the Pareto surface will always sacrifice the quality for at least one objective, while improving the other objective. Here we have used two different methods to create a Pareto optimal surface namely Multi-Objective Genetic Algorithm (MOGA) and Non-Linear Programming by Quadratic Lagrangian (NLPQL).

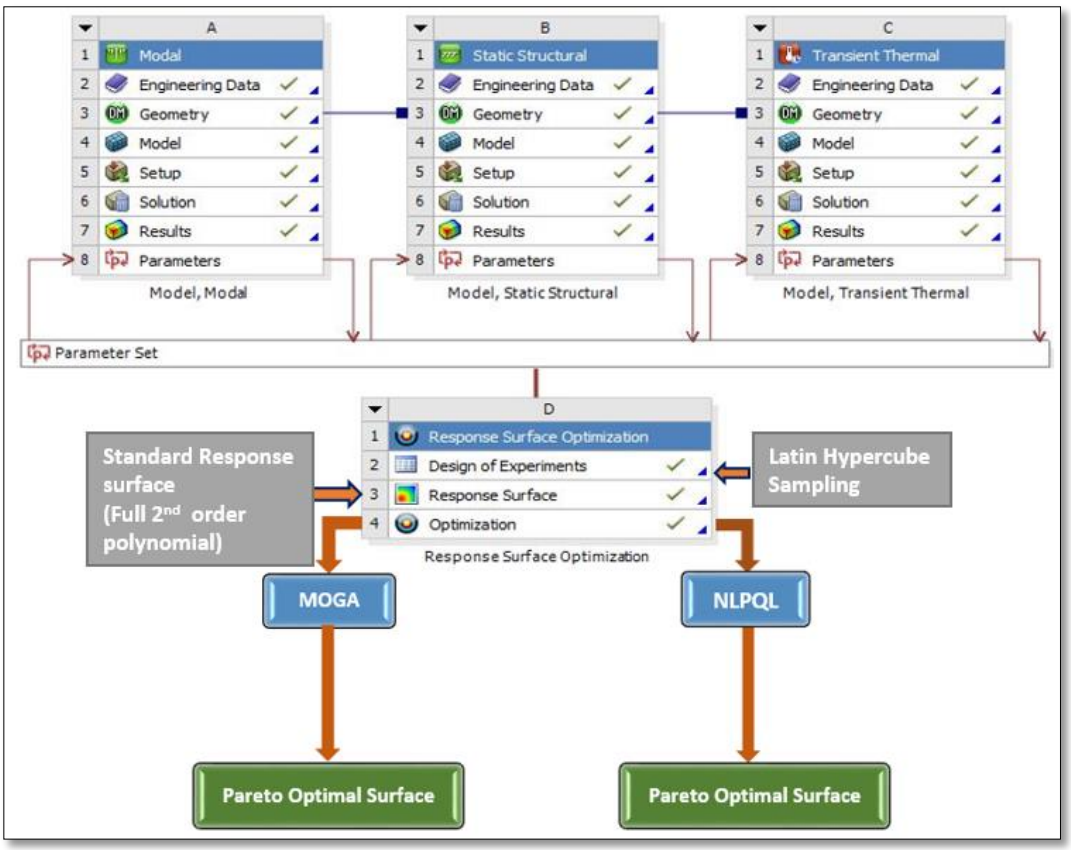

Figure 47: System Optimization schematic diagram

7.1 Multi-Objective Genetic Algorithm (MOGA)

MOGA is a hybrid variant of the popular NSGA-II (Non-dominated Sorted Genetic Algorithm). Only continuous problems can be solved using the same. The Algorithm goes through several iterations retaining the elite percentage of samples through each iteration and allowing the samples to evolve genetically until the best Pareto has been found. As mentioned above this method can handle multiple goals. Some of the other advantages are it helps identify the global and local minima of the function. It also provides several candidates in different regions giving accurate solutions.

7.1.1 Optimization Process

The following steps were taken to generate the Pareto optimal surface using MOGA.

1. Three subsystems were integrated with the common input parameters as design variables and the output as state variables.
2. Design of experiments was performed using Latin Hypercube Sampling (LHS)
3. A second order polynomial response surface was created from the DOE samples generated.
4. Optimal solutions were generated from the response surface using MOGA
5. The deviation in the predicted value from the MOGA optimization and the simulated value was corrected.
6. A Pareto optimal surface was generated using least squares regression analysis.

7.1.2 Results

The figure 47 shows the Pareto surface obtained from MOGA optimization. The non-pareto points are not considered for generating the surface.

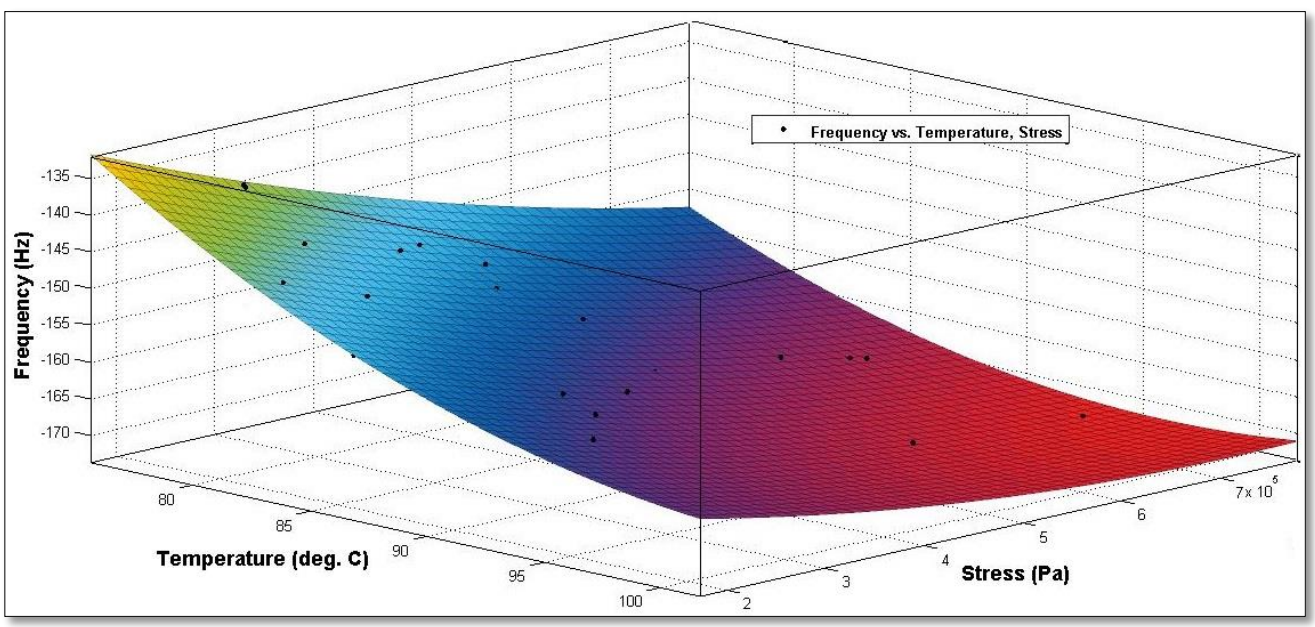

Figure 48: MOGA Pareto Surface

7.2 Non-Linear Programming by Quadratic Lagrangian (NLPQL)

NLPQL is a mathematical optimization Algorithm which solves non-linear programming problems. In this method the objective function and the constraints are assumed to be continuously differentiable. Here a sequence of QP sub problems are obtained by quadratic approximation of the Lagrangian function. The problem size cannot exceed 2000 input variables and has to be well scaled. Though the method is fast, the accuracy largely depends on the accuracy of the gradients. This is primarily used for single objective problems but can also be used for multi-objective problems by constraining the other output parameters.

7.2.1 Optimization Process

The following steps were taken to generate the Pareto optimal surface using NLPQL.

1. Three subsystems were integrated with the common input parameters as design variables and the output as state variables.
2. Design of experiments was performed using Latin Hypercube Sampling (LHS)
3. A second order polynomial response surface was created from the DOE samples generated.
4. Optimal solutions were generated by considering output frequency (maximize) from the modal analysis as objective and constraining the other two output parameters.
5. The deviation in the predicted value from the NLPQL optimization and the simulated value was corrected.
6. A Pareto optimal surface was generated using least squares regression analysis.

7.2.2 Results

The figure 48 shows the Pareto surface obtained from NLPQL optimization. The non-pareto points are not considered for generating the surface.

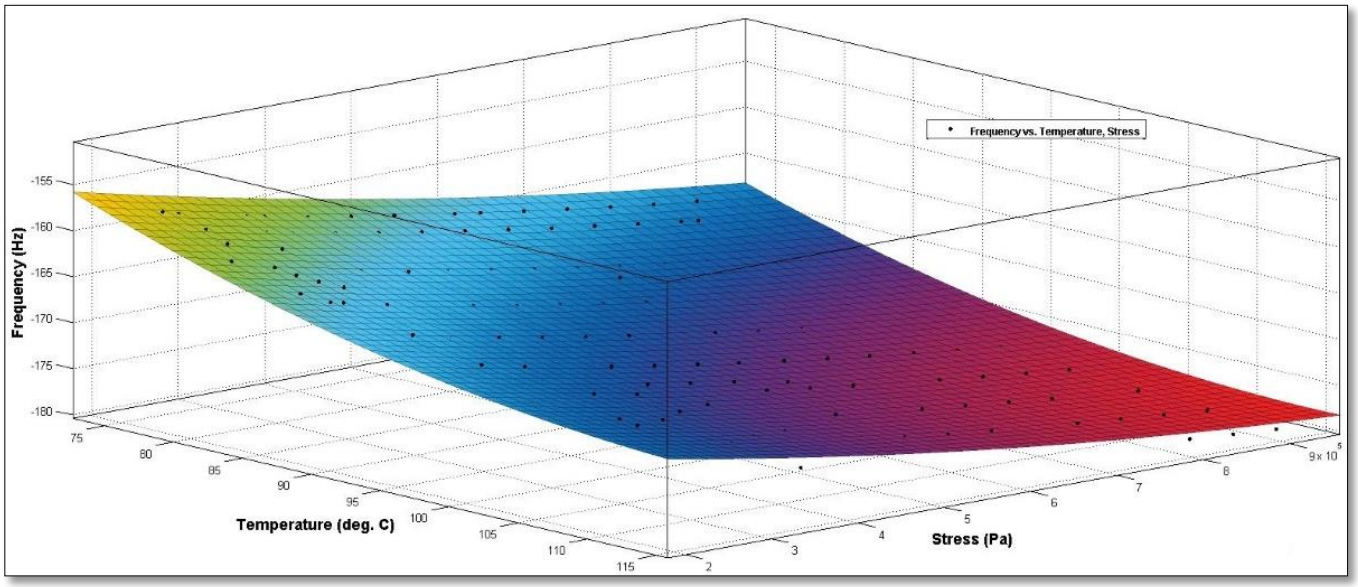

Figure 49: NLPQL Pareto Surface

7.3 Conclusion

The Pareto surfaces obtained from the optimization methods MOGA and NLPQL are very much comparable. There is no single point which serves as the best value for all objectives (Utopia point).To get an ideal point from the Pareto surface for a particular application the subsystem objectives need to be weighted. But in this project we have weighted all the objective equally.

8 References

1. http://mostreal.sk/html/guide_55/g-adv/GADV1.htm
2. http://inside.mines.edu/~apetrell/ENME442/Labs/1301_ENME442_lab5.pdf
3. Dr. Max Yi Ren, Notes for MAE 598: Design Optimization
4. How a car clutch works By Mike Bumbeck, automedia.com
5. http://www.dynardo.de/fileadmin/Material_Dynardo/dokumente/seminar/Doku_Bearing_Angle_English_v12.pdf
6. http://www.hindawi.com/journals/isrn/2013/495918/
7. http://www.ansys.com/staticassets/ansys/conference/confidence/boston/downloads/obtaining-and-optimizing-convergence.pdf
8. Design Optimization of the Rigid Drive Disc of Clutch Using Finite Element Method
9. Abdullah, O., Schlattmann, J., and Pireci, E., "Design Optimization of the Rigid Drive Disc of Clutch Using Finite Element Method," SAE Technical Paper 2014-01-0800, 2014, doi:10.4271/2014-01-0800.
10. ANSYS. (2009). *Design Exploration.* Canonsburg: ANSYS.

9 APPENDIX

DOE SAMPLE SPACE FOR SUB SYSTEM OPTMIZATION

Modal Analysis

Matrix of Experiments (Response Surface Optimization system)

Name	P29 - Plane4.D2 (mm)	P30 - Extrude1.FD1 (mm)	P31 - Extrude2.FD1 (mm)	P39 - Total Deformation Reported Frequency (Hz)
1	149	7.2	0.55	152.73
2	152.33	7.7333	1.95	141.94
3	140.33	5.0667	2.15	163.13
4	150.33	8.8	2.95	136.61
5	141.67	4	1.25	170.42
6	158.33	2.1333	3.45	157.74
7	149.67	9.3333	1.65	139.13
8	157.67	9.0667	3.15	129.73
9	145	5.8667	1.35	157.56
10	143.67	9.8667	2.75	136.91
11	146.33	5.6	2.45	153.76
12	143	4.5333	0.95	167.75
13	148.33	6.1333	3.05	148.03
14	153.67	2.4	1.45	169.29
15	145.67	8.5333	2.05	143.17
16	156.33	5.3333	1.85	150.61
17	155.67	8.2667	1.05	141.19
18	151.67	4.8	0.85	160.74
19	142.33	3.7333	1.75	169.57
20	141	3.4667	2.85	166.58
21	147.67	2.6667	3.35	162.8
22	157	6.6667	2.65	140.8
23	159	8	1.55	138.81
24	144.33	6.9333	2.35	148.97
25	154.33	2.9333	3.25	157.66
26	151	4.2667	0.65	165.56
27	155	7.4667	2.25	140.7
28	153	6.4	1.15	151.27
29	159.67	3.2	0.75	165.33
30	147	9.6	2.55	136.74
1	140	2	0.5	179.85

Structural Analysis

Matrix of Experiments (Response Surface Optimization system)

Name	P32 - Plane4.D2 (mm)	P33 - Extrude1.FD1 (mm)	P34 - Extrude2.FD1 (mm)	P27 - Equivalent Stress Maximum Maximum Value Over Time (Pa)
1	149	7.2	0.55	5.3691E+05
2	152.33	7.7333	1.95	2.954E+05
3	140.33	5.0667	2.15	5.373E+05
4	150.33	8.8	2.95	2.9526E+05
5	141.67	4	1.25	8.6594E+05
6	158.33	2.1333	3.45	2.5624E+05
7	149.67	9.3333	1.65	2.891E+05
8	157.67	9.0667	3.15	2.1205E+05
9	145	5.8667	1.35	4.7106E+05
10	143.67	9.8667	2.75	3.6161E+05
11	146.33	5.6	2.45	4.3942E+05
12	143	4.5333	0.95	7.4132E+05
13	148.33	6.1333	3.05	3.7093E+05
14	153.67	2.4	1.45	4.4319E+05
15	145.67	8.5333	2.05	3.2724E+05
16	156.33	5.3333	1.85	2.5037E+05
17	155.67	8.2667	1.05	2.7078E+05
18	151.67	4.8	0.85	3.9925E+05
19	142.33	3.7333	1.75	6.5393E+05
20	141	3.4667	2.85	7.6878E+05
21	147.67	2.6667	3.35	5.9855E+05
22	157	6.6667	2.65	2.112E+05
23	159	8	1.55	2.1179E+05
24	144.33	6.9333	2.35	4.2676E+05
25	154.33	2.9333	3.25	3.1613E+05
26	151	4.2667	0.65	5.6137E+05
27	155	7.4667	2.25	2.3842E+05
28	153	6.4	1.15	3.1823E+05
29	159.67	3.2	0.75	2.8779E+05
30	147	9.6	2.55	2.9608E+05

Thermal Analysis

Matrix of Experiments (Response Surface system)

Name	P21 - lining_thickness.FD1 (mm)	P23 - plate_thickness.FD1 (mm)	P24 - Plane4.D2 (mm)	P14 - Temperature Maximum Maximum Value Over Time (C)
1	2.075	3.8	153.54	105.13
2	2.675	7.4	142.51	84.337
3	0.575	7.8	145.52	120.39
4	2.375	2.2	144.51	87.456
5	0.875	5	157.55	110.07
6	3.425	5.4	154.54	82.26
7	2.225	7	158.56	92.246
8	3.275	6.2	148.53	77.799
9	1.475	9.4	140.5	85.664
10	1.325	2.6	143.51	113.49
11	1.775	5.8	141.5	116.04
12	1.175	6.6	155.55	122.62
13	1.925	4.6	159.56	97.903
14	2.825	8.2	149.53	78.839
15	1.625	3	146.52	99.265
16	3.125	3.4	151.53	80.286
17	2.975	9.8	152.54	83.023
18	2.525	8.6	150.53	91.585
19	1.025	4.2	147.52	116.37
20	0.725	9	156.55	112.13
21	3.5	6.001	150.03	73.69
22	3.5	6	150.03	75.462
1	2	6	150.03	98.997
2	3.4533	6	150.03	78.789

Matrix of Experiments (Response Surface Optimization system)

Name	P29 - Plane4.D2 (mm)	P30 - Extrude1.FD1 (mm)	P31 - Extrude2.FD1 (mm)	P27 - Equivalent Stress Maximum Maximum Value Over Time (Pa)	P28 - Temperature Maximum Maximum Value Over Time (C)	P39 - Total Deformation Reported Frequency (Hz)
1	149	7.2	0.55	5.1623E+05	116.86	152.73
2	152.33	7.7333	1.95	2.9538E+05	100.52	141.94
3	140.33	5.0667	2.15	5.373E+05	95.998	163.13
4	150.33	8.8	2.95	2.8692E+05	74.566	136.61
5	141.67	4	1.25	8.6594E+05	110.46	170.42
6	158.33	2.1333	3.45	2.5624E+05	72.728	157.74
7	149.67	9.3333	1.65	2.8946E+05	102.35	139.13
8	157.67	9.0667	3.15	2.1557E+05	73.862	129.73
9	145	5.8667	1.35	4.7106E+05	88.675	157.56
10	143.67	9.8667	2.75	3.396E+05	82.32	136.91
11	146.33	5.6	2.45	4.3942E+05	77.564	153.76
12	143	4.5333	0.95	7.4132E+05	112.19	167.75
13	148.33	6.1333	3.05	3.7093E+05	77.057	148.03
14	153.67	2.4	1.45	4.4319E+05	98.23	169.29
15	145.67	8.5333	2.05	3.2912E+05	72.54	143.17
16	156.33	5.3333	1.85	2.5037E+05	87.657	150.61
17	155.67	8.2667	1.05	2.7408E+05	111.97	141.19
18	151.67	4.8	0.85	4.3361E+05	111.97	160.74
19	142.33	3.7333	1.75	6.5393E+05	96.797	169.57
20	141	3.4667	2.85	7.6878E+05	93.193	166.58
21	147.67	2.6667	3.35	5.9855E+05	74.404	162.8
22	157	6.6667	2.65	2.112E+05	77.642	140.8
23	159	8	1.55	2.1216E+05	85.363	138.81
24	144.33	6.9333	2.35	4.2676E+05	93.05	148.97
25	154.33	2.9333	3.25	3.1613E+05	80.642	157.66
26	151	4.2667	0.65	5.6137E+05	113.28	165.56
27	155	7.4667	2.25	2.385E+05	96.585	140.7
28	153	6.4	1.15	3.1803E+05	116.03	151.27
29	159.67	3.2	0.75	2.8779E+05	113.79	165.33
30	147	9.6	2.55	2.9594E+05	84.599	136.74
32	160	10	2.52	1.8911E+05	86.093	128.39

Frequency Table for NLPQL optimization

	116.8597	111.86	106.86	101.86	96.86	91.86	86.86	81.86	76.86
865936.4	177.6863	177.3201	176.8206	176.0993	175.0604	173.6128	171.6858	168.8803	168.0506
815936.4	177.3113	162.5282	176.3479	175.5883	174.5206	173.055	171.122	168.6539	167.5011
765936.4	176.9213	176.4468	175.8511	175.0495	173.9501	172.4649	170.5253	168.0654	166.9204
464139.2	176.5141	175.9813	175.3301	174.4673	173.348	171.8411	169.8945	167.4437	166.3076
464139.2	162.5282	175.4977	162.5282	173.8869	172.714	171.1616	169.2119	166.7887	165.6624
464139.2	175.6316	174.9927	174.2208	173.2649	172.049	170.4919	168.5294	166.101	164.9859
562079.3	175.1461	173.3298	173.6337	172.5865	171.125	169.77	167.7984	165.3839	164.5663
507249.4	174.6223	173.8914	173.0161	171.9516	170.6417	169.0237	167.0424	164.6433	163.5544
456552.6	174.0514	171.8482	171.8482	171.2472	169.8971	168.2514	166.2609	163.8742	162.7962
415568.9	173.0372	172.0405	171.1161	170.4926	169.1067	167.4364	165.4369	163.0596	161.9905
362596.5	172.446	171.4846	170.8603	169.35	168.2512	162.8555	164.55	162.1796	161.1179
315936.4	171.9203	171.0267	169.9832	168.7561	167.45	165.592	162.0338	161.6101	160.7216
265936.4	170.3167	170.063	168.4536	167.718	166.2383	164.5031	162.4759	160.1134	159.0627
215936.6	162.8411	162.8411	162.8411	162.8411	162.8411	162.6585	160.9297	157.3006	155.21
211203.7	160.7008	160.7008	162.8411	160.7008	160.6785	160.5906	158.9318	155.1963	152.9876

stress

Temperature

Stress Table for NLPQL optimization

116.8597	111.86	106.86	101.86	96.86	91.86	86.86	81.86	76.86
116.8597	111.86	94.47533	101.86	96.86	91.86	86.86	81.86	76.86
116.8597	111.86	106.86	101.86	96.86	91.86	86.86	81.86	76.86
94.47533	111.86	106.86	101.86	96.86	91.86	86.86	81.86	76.86
94.47533	94.47533	106.86	94.47533	96.86	91.86	86.86	81.86	76.86
94.47533	111.86	106.86	101.86	96.86	91.86	86.86	81.86	76.86
100.4917	111.86	100.4917	101.86	96.86006	90.73919	86.86	81.86	76.86
100.0483	111.86	106.86	101.86	96.86	91.86	86.86	81.86	76.86
100.0535	111.86	100.0535	100.0535	96.86	91.86	86.86	81.86	76.86
113.9819	109.465	104.0225	100.098	96.86	91.86	86.86	81.86	76.86
113.4395	110.3675	105.1997	101.86	90.73919	91.86	86.12637	81.86	76.86
116.86	111.86	106.86	101.86	96.86	91.69632	86.86	79.54861	76.86
108.1493	108.1493	106.86	93.1717	96.86	91.86	86.86	81.86001	76.86
89.04096	89.04096	89.04096	89.04096	89.04096	89.0411	86.86	81.86	76.86
88.48115	88.48115	88.48115	89.04096	88.48115	90.33979	86.86	81.86	76.86

Temperature Table for NLPQL optimization

116.8597	111.86	106.86	101.86	96.86	91.86	86.86	81.86	76.86
116.8597	111.86	94.47533	101.86	96.86	91.86	86.86	81.86	76.86
116.8597	111.86	106.86	101.86	96.86	91.86	86.86	81.86	76.86
94.47533	111.86	106.86	101.86	96.86	91.86	86.86	81.86	76.86
94.47533	94.47533	106.86	94.47533	96.86	91.86	86.86	81.86	76.86
94.47533	111.86	106.86	101.86	96.86	91.86	86.86	81.86	76.86
100.4917	111.86	100.4917	101.86	96.86006	90.73919	86.86	81.86	76.86
100.0483	111.86	106.86	101.86	96.86	91.86	86.86	81.86	76.86
100.0535	111.86	100.0535	100.0535	96.86	91.86	86.86	81.86	76.86
113.9819	109.465	104.0225	100.098	96.86	91.86	86.86	81.86	76.86
113.4395	110.3675	105.1997	101.86	90.73919	91.86	86.12637	81.86	76.86
116.86	111.86	106.86	101.86	96.86	91.69632	86.86	79.54861	76.86
108.1493	108.1493	106.86	93.1717	96.86	91.86	86.86	81.86001	76.86
89.04096	89.04096	89.04096	89.04096	89.04096	89.0411	86.86	81.86	76.86
88.48115	88.48115	88.48115	89.04096	88.48115	90.33979	86.86	81.86	76.86

MATLAB CODE FOR REGRESSION ANALYSIS FOR MOGA

```
clc

clear all

A = xlsread('opti.xlsx');

Y = -A(:,3);

X1 = A(:,1);

X2 = A(:,2);

beta0 = ones(50,1);
```

```
X = [X1 X2 beta0 (X1.^2) (X2.^2) (X1.*X2)];

z = inv(X'*X);

b = z*X'*Y;

x1 = [0:0.01:1];

x2 = 0:0.01:1;

[X1,X2] = meshgrid(x1,x2);

for i = 1:length(x1)

    for j = 1:length(x2)

        y(i,j) =
b(1)*x1(i)+b(2)*x2(j)+b(3)+b(4)*x1(i)^2+b(5)*x2(j)^2+b(6)*x1(i)*x2(j);

    end

end

surf(X1,X2,y);

xlabel('stress');ylabel('temp');zlabel('freq');
```

FREQUENCY-STRESS-TEMPERATURE TABLE (A) FOR REGRESSION ANALYSIS

Stress	Temperature	Frequency
895533.4214	83.18674111	168.5236306
652192.6985	85.93746706	167.6086429
621110.1679	86.13590557	165.5054552
685991.8803	90.96025367	170.5626591
673166.8557	87.61590634	166.2201614
657732.531	87.55078208	165.719328
302136.8415	81.21101819	157.8928123
438377.6904	81.70168443	158.0300236
289841.0455	81.89792073	158.0666637
737797.2284	94.11994465	171.4861478
481203.7145	86.65509461	162.8515439
473842.365	79.32038087	154.5857633
473085.4585	79.32038087	154.5607684
665677.9682	95.09799417	171.961458
417880.7784	87.90464731	163.1505045
457002.4378	78.53251736	152.712077
307965.2356	85.01967817	159.8649554
404709.3716	87.8755653	162.7579958
459408.5024	80.82121938	154.886515
421856.2728	79.32038087	152.8688587
473432.1719	83.93442786	157.3095171
548504.5337	94.86687358	168.8477205
401095.0935	88.88789379	161.5447877
297958.4156	80.58952886	151.5796391
429991.1465	78.77550798	149.4955515
429991.1465	78.77550798	149.4955515
336087.7617	88.88789379	159.8708133
264219.1465	87.94674043	157.1472155
425490.3686	81.78457336	149.9077393
209505.3171	80.58952886	148.5409389
418061.5303	99.43655218	169.3828325
418929.3845	99.6224907	169.447168
257164.8734	92.17404728	161.0075767
228545.6073	86.51849366	153.8341808
293182.9648	92.09552751	159.1107927
299530.6584	79.39109788	144.9571376

299530.6584	79.39109788	144.9571376
276177.3034	83.04607476	148.8294811
348378.3708	81.41618407	145.9315487
303601.6682	76.69006994	139.2289415
208905.6281	82.29921414	145.4102032
232589.9871	94.55917933	158.9532526
302112.1589	76.66877224	138.9050244